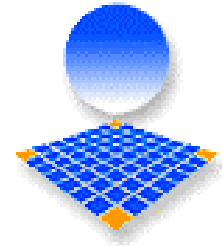




An IMI Video Reproduction of Invited Lectures
from the 17th University Glass Conference



Université Montpellier II

Ion diffusion in chalcogenide glasses Application in ionics and optics

Michel RIBES and Annie PRADEL

Laboratoire de Physicochimie de la Matière Condensée

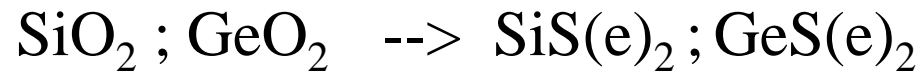
UMR 5617 CNRS

Université Montpellier II, Montpellier FRANCE

Chalcogenide Glasses

Chalcogenide glasses are glasses containing chalcogens (Se, S, Te).

Chalcogenide homologous of oxide glasses



Ia																			0	
1 H	IIa												IIIa	IVa	Va	VIa	VIIa	2 He		
3 Li	4 Be												5 B	6 C	7 N	8 O	9 F	10 Ne		
11 Na	12 Mg	IIIb	IVb	Vb	VIb	VIIB	VIIIb			Ib	IIb	13 Al	14 Si	15 P	16 S	17 Cl	18 Ar			
19 K	20 Ca	21 Sc	22 Ti	23 V	24 Cr	25 Mn	26 Fe	27 Co	28 Ni	29 Cu	30 Zn	31 Ga	32 Ge	33 As	34 Se	35 Br	36 Kr			
37 Rb	38 Sr	39 Y	40 Zr	41 Nb	42 Mo	43 Tc	44 Ru	45 Rh	46 Pd	47 Ag	48 Cd	49 In	50 Sn	51 Sb	52 Te	53 I	54 Xe			
55 Cs	56 Ba	57 La	72 Hf	73 Ta	74 W	75 Re	76 Os	77 Ir	78 Pt	79 Au	80 Hg	81 Tl	82 Pb	83 Bi	84 Po	85 At	86 Rn			
87 Fr	88 Ra	89 Ac	104 Unq	105 Unp	106 Unh	107 Uns														
							58 Ce	59 Pr	60 Nd	61 Pm	62 Sm	63 Eu	64 Gd	65 Tb	66 Dy	67 Ho	68 Er	69 Tm	70 Yb	71 Lu
							90 Th	91 Pa	92 U	93 Np	94 Pu	95 Am	96 Cm	97 Bk	98 Cf	99 Es	100 Fm	101 Md	102 No	103 Lr

Chalcogenide Glasses

Presence of S, Se, Te --> polarisable environment
with lone-pair (LP)



Specific property of chalcogenide glasses compared to
oxide ones

They exhibit semiconductor properties and thus form a large group of
amorphous semiconductors

Intrinsically metastable, they can undergo various structural
transformations under the action of external stimuli, in particular light.

Semiconductor

As_2S_3 glass

$\sigma \sim 10^{-14} \text{ Scm}^{-1}$

$E_g \sim 2,15 \text{ eV}$

Photoinduced phenomena

$h\nu \rightarrow$ hole-electron pair \rightarrow change in n

Ovshinsky effect

(amorphous state \leftrightarrow crystalline state)

Transparency in the IR

Application of ion diffusion in chalcogenide glasses

☰ Interface ion exchange

➔ Ion sensors

☰ Diffusion under \vec{E}

➔ Electrochemical energy storage : batteries

☰ Diffusion under photons $h\nu$

➔ Photoinduced phenomena

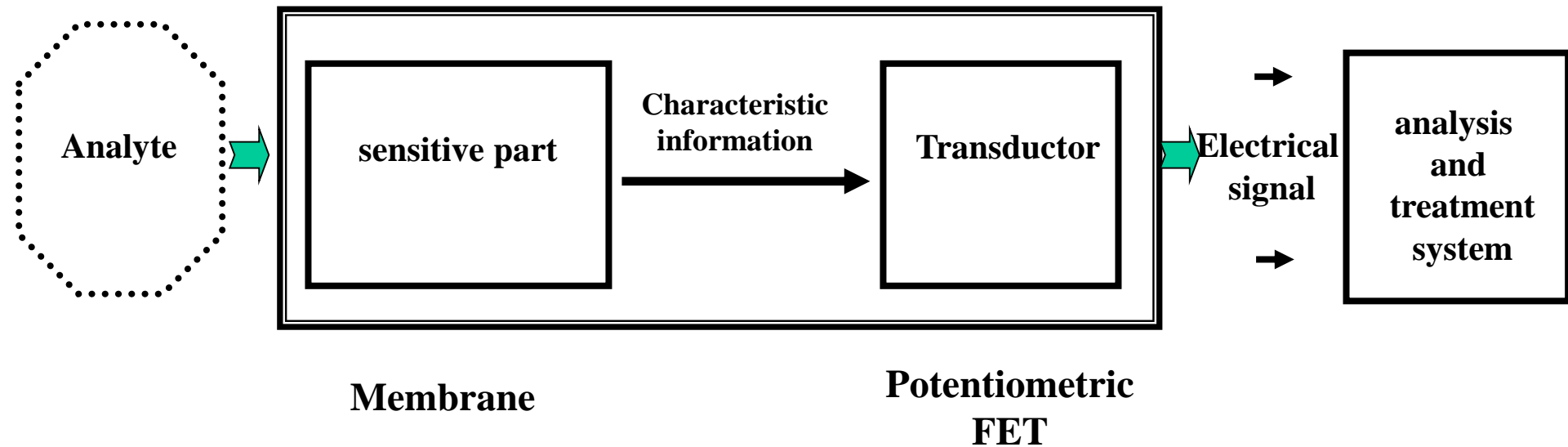
☰ Diffusion under \vec{E} and $h\nu$

➔ PMC memories

Ion exchange : Chemical Sensor

Principle of a sensor

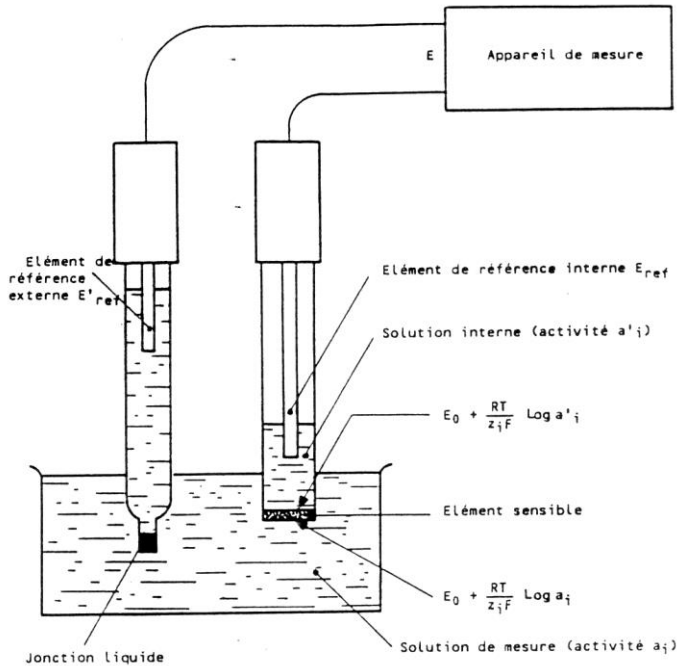
CHEMICAL or PHYSICAL SENSOR



Sensitivity, reversibility, selectivity and stability

Ion-selective electrode

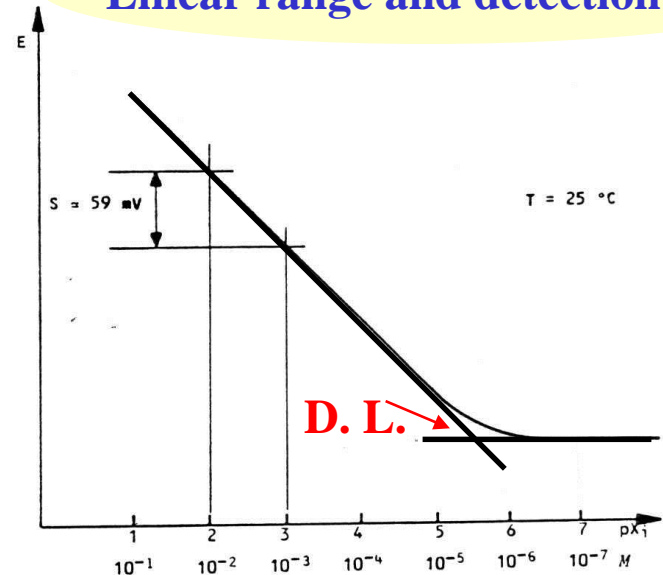
determination of e.m.f between the ISE and a reference electrode.



Potentiometric analysis of a chemical sensor depends on the relationship between the concentration of the species and the e.m.f. The ideal relationship is known as the Nernst equation :

$$E = E_0 + \frac{RT}{z_i F} \text{Log } a_i$$

Linear range and detection limit

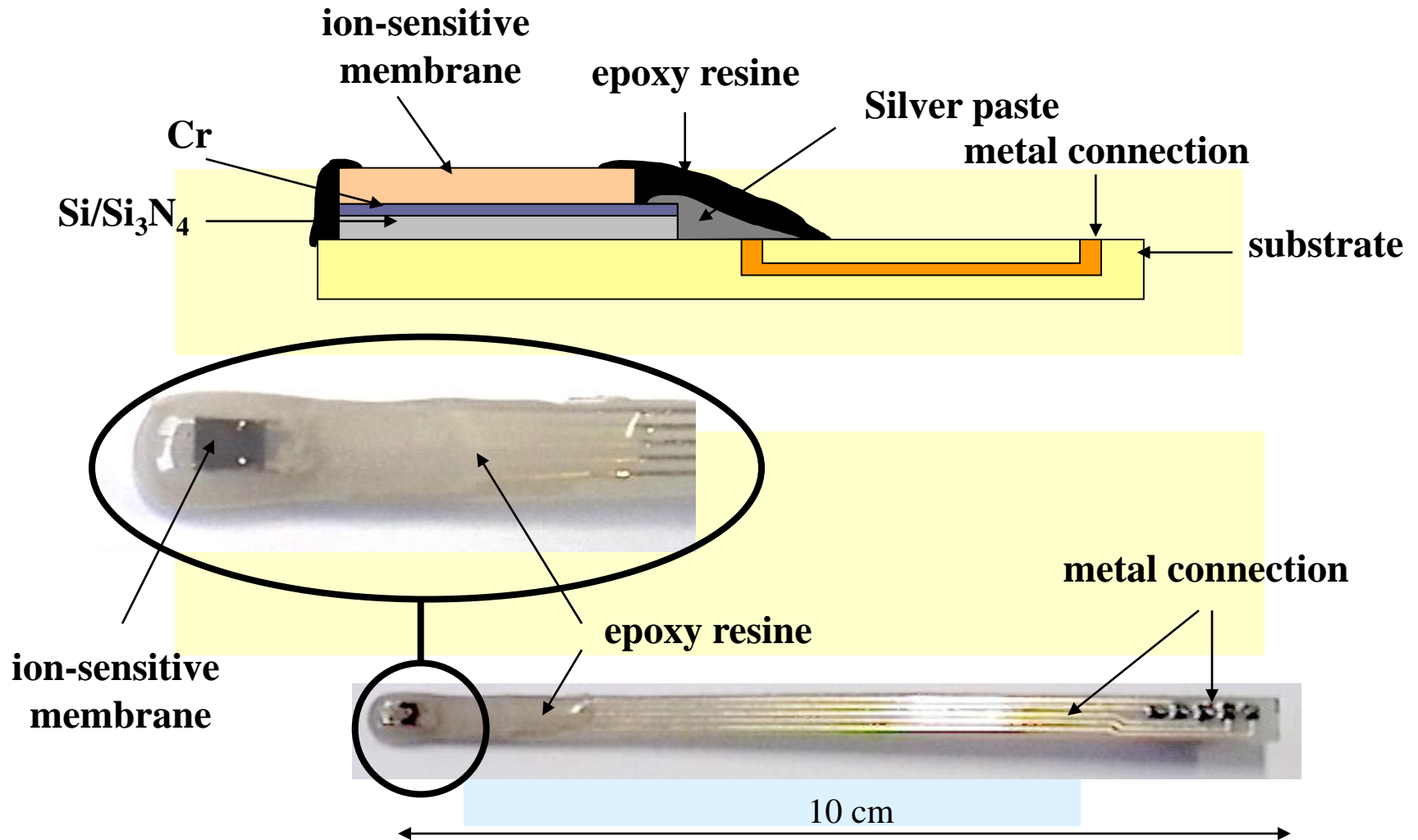


Slope of the response

Typical calibration curve of an ion-selective electrode obtained with the well known addition method.

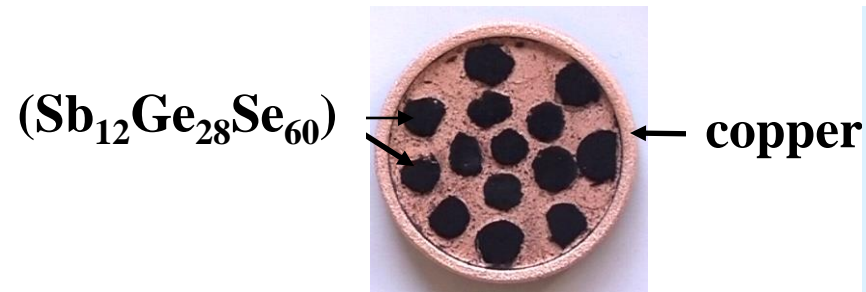
Development of ISE chemical microsensors

Analytical device for Cu^{2+} ion detection based on $(1-X)\text{Sb}_{12}\text{Ge}_{28}\text{Se}_{60} - X\text{Cu}$ glassy thin films.



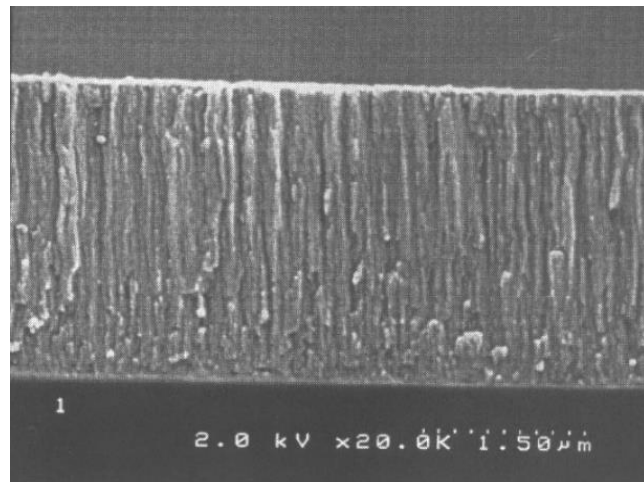
Elaboration of the (Sb-Ge-Se)/(Cu) material

Thin films produced by r.f. sputtering of a composite target



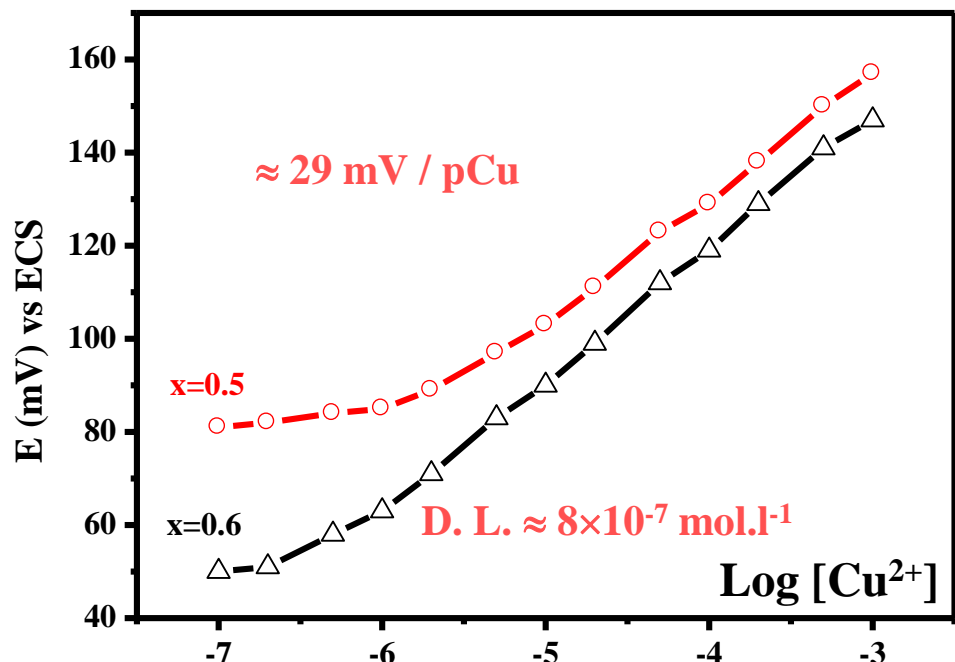
Target	Chemical composition of thin films
1	$(\text{Sb}_{11.3}\text{Ge}_{30.4}\text{Se}_{58.3})_{40}(\text{Cu})_{60}$
2	$(\text{Sb}_{11}\text{Ge}_{29}\text{Se}_{60})_{50}(\text{Cu})_{50}$

S.E.M cross sectional view of a thin film



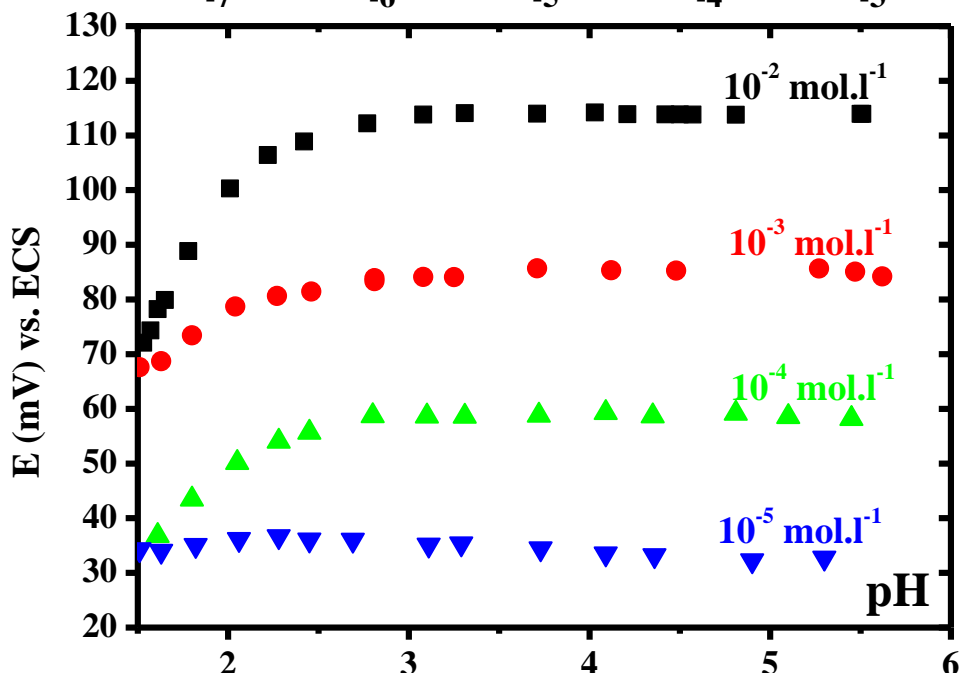
Film thickness varies from 0.4 to 1 μm depending on sputtering conditions and sputtering time.

Electrode response



The material with $x = 0.6$ gives the best electrode performance.

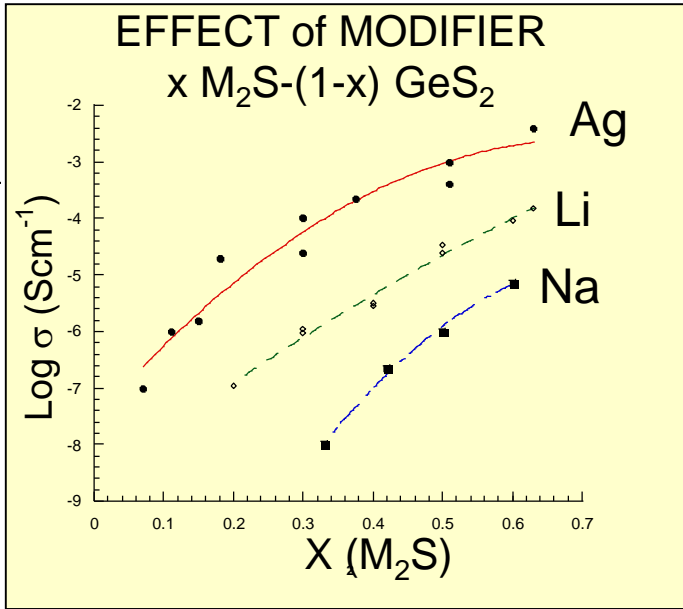
Mixed solution method with constant a interfering ion concentration.



Interfering Ion	$\log K_{\text{Cu}^{2+}/j}$
K^+	-5.1
Na^+	-5.3
Ca^{2+}	-5.1
Ni^{2+}	-4.1
Cd^{2+}	-4.1
Pb^{2+}	-2.5
Mn^{2+}	-3.4

Influence of pH on electrode response

Diffusion under \vec{E} : chemical energy storage



Superionic Conductive Glasses

Conductivity 100-1000 times larger than that of their oxide counterpart

$\epsilon_r > 10$ (Weak electrolyte theory)

$$\sigma_{Ag^+} \sim 10^{-2} Scm^{-1}$$

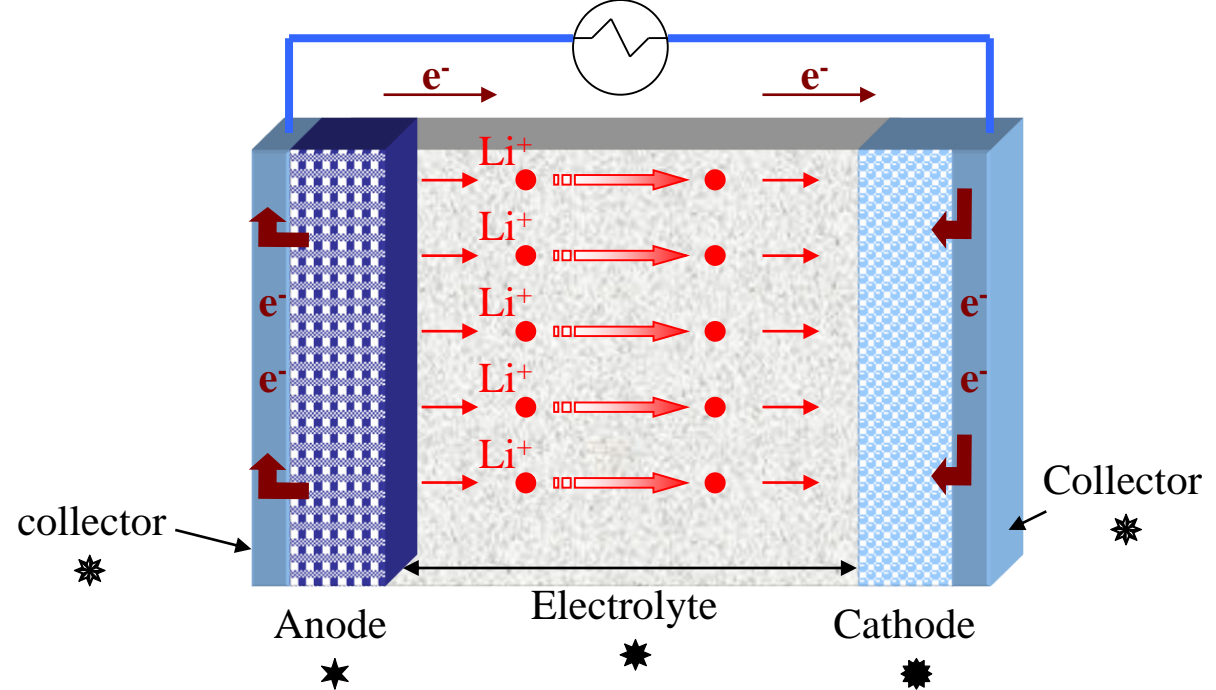
$$\sigma_{Li^+} \sim 10^{-3} Scm^{-1}$$

Application: all solid state batteries based on solid electrolytes

Rocking-chair Li-ion batteries for various portable equipments

- Safety: prevent from igniting and leaking (liquid combustible organic solvent)
- miniaturisation

Li-ion battery



At the beginning: Li batteries

- ✓ our first works (1983) $\text{Li/LiI-Li}_2\text{S-GeS}_2(\text{g})/\text{V}_2\text{O}_5$
- ✓ Eveready (USA)(90 's) $\text{Li/ sulfide (oxysulfide) (g)/various cathodic materials}$

Now Li-ion batteries (mainly japanese teams)

- ✓ Minami-Tatsumisago group (Osaka)
 $\text{In/Li}_2\text{S-P}_2\text{S}_5\text{glass-ceramics/LiCoO}_2$ (Chem.Letters 2002)
- ✓ Takada et al (NIMS-Tsukuba)
 $\text{C/Li-Li}_2\text{S-P}_2\text{S}_5(\text{g})//\text{Li}_3\text{PO}_3\text{-Li}_2\text{S-SiS}_2(\text{g})/\text{LiCoO}_2$ (SSI 2003)

Li (or Li-ion) microbattery

Reduction of power supply of electronics devices

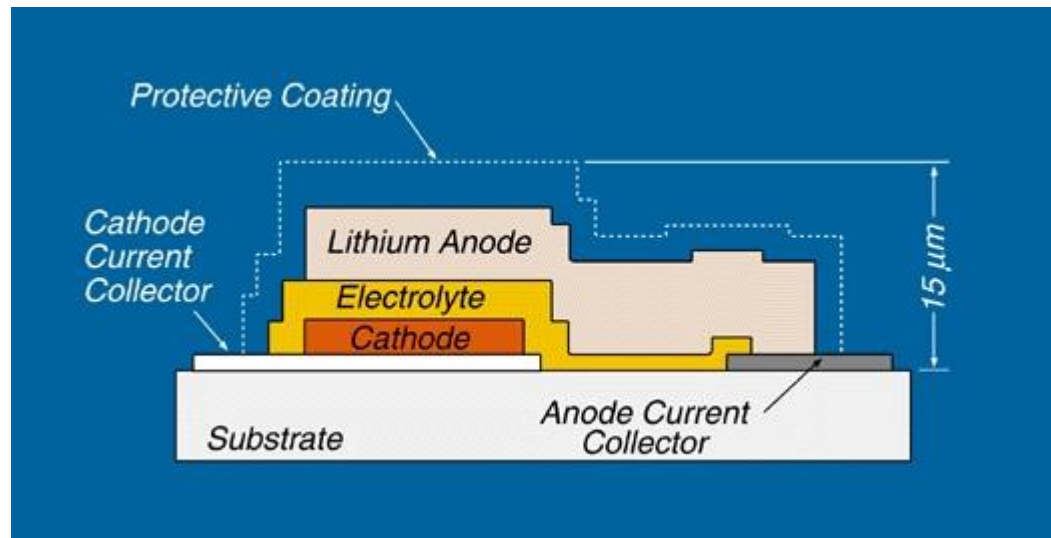
☰ Active power sources:

implantable medical devices, remote sensors, miniature transmitters, smart cards

☰ Standby power sources:

CMOS-SRAM memory devices (few $\text{mWh}\cdot\text{cm}^{-2}$ are required to back up a CMOS memory chip)

Thin-films lithium battery developed at ORNL



Neudecker BJ, Dudney NJ and Bates JB ; J. Electrochem. Soc. 147 (2000) 517

Levasseur group Bordeaux Fr; Industrialization HEF Group (SVF Gazette du Vide 2 march 2003)

Diffusion under photons $h\nu$: Photoinduced phenomena

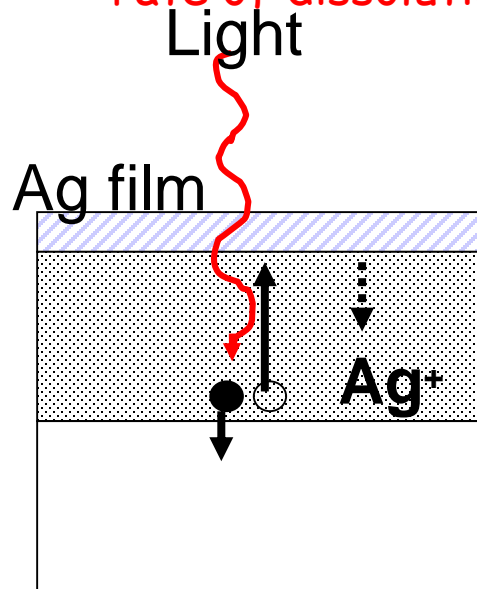
Photodissolution (« photodoping »)

Illumination of a chalcogenide film in contact with silver

-> rapid penetration of the metal into the semiconductor (Kostyshin (1966))

Typical features :

- large amount of Ag can be dissolved 30-40 at%, and even 57% in GeS_3
- rate of dissolution depends on chalcogenide composition (excess in chalcogen)



Mechanism

ionization of Ag

(semiconductor \rightarrow presence of holes or electrons)



reduction of chalcogenide



$h\nu$ close to bandgap energy

Photo-enhanced solid state reaction

Application of photodissolution

Very sharp edges between doped and undoped regions

Local creation of pairs « electron-hole » + small diffusion length of free carriers

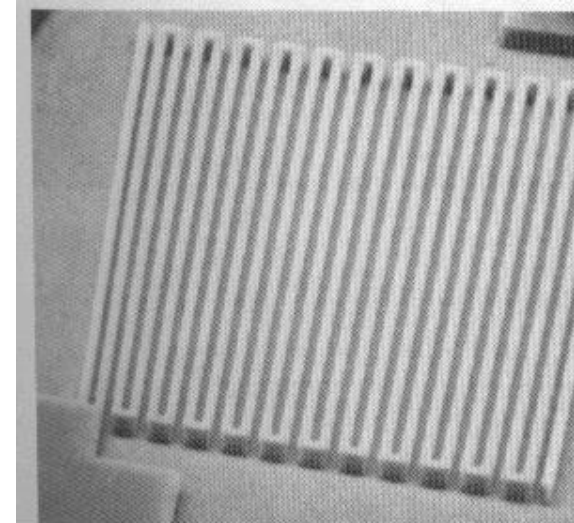
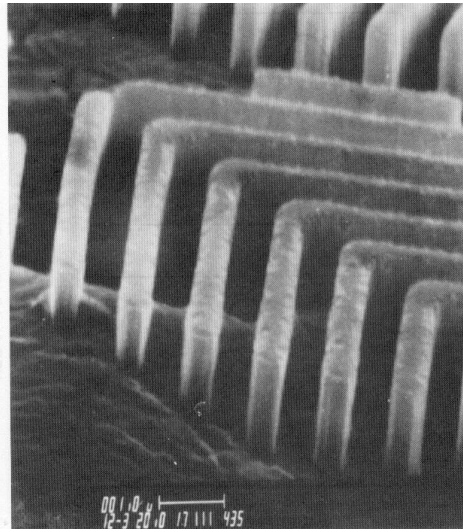
↓
Hardly any lateral diffusion

Solubility of doped region in alkaline solvents much reduced

Local change in chemical composition

photoresists →

etched gratings



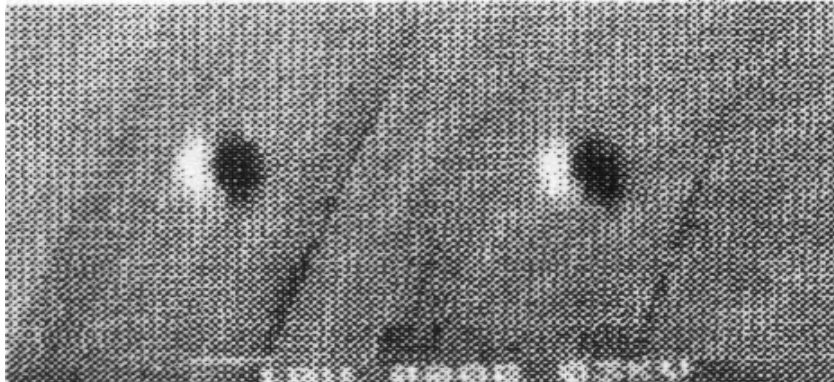
Photomigration - Photodeposition

Phenomenon observed in highly doped chalcogenide: Ag-Ge-S(e), Ag-As-S(e). For example in $(\text{Ge}_{0.3}\text{S}_{0.7})_{100-x}\text{Ag}_x$ films when $x > 0.45$

Illumination

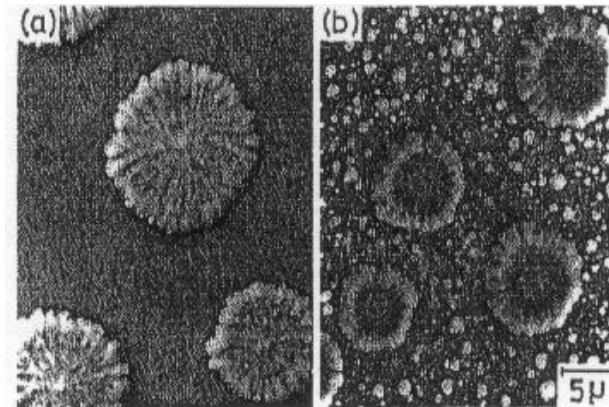
lower silver content ($x < 0.45$)

increase in Ag density
in the illuminated part



higher silver content ($\text{Ag}_{45}\text{As}_{15}\text{S}_{40}$)

precipitation of Ag



200mW/cm²

530mW/cm²

Small clusters or crystals
10nm in diameter and 1nm in thickness

Reversible process

Annealing → dissolution of the Ag clusters

Mechanism of photomigration-photodeposition

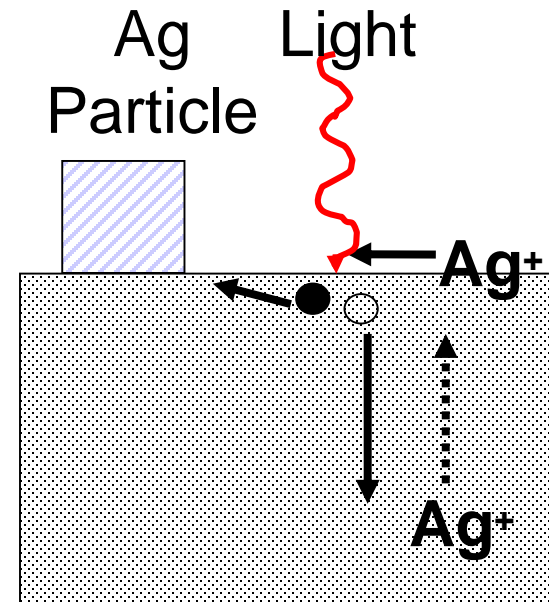
Point of view of physicist

Illumination

creation of pair « electron-hole »



h^+ moves away from illuminated spot



Point of view of chemist

Photodecomposition = decomposition of an oversaturated Ag solid solution

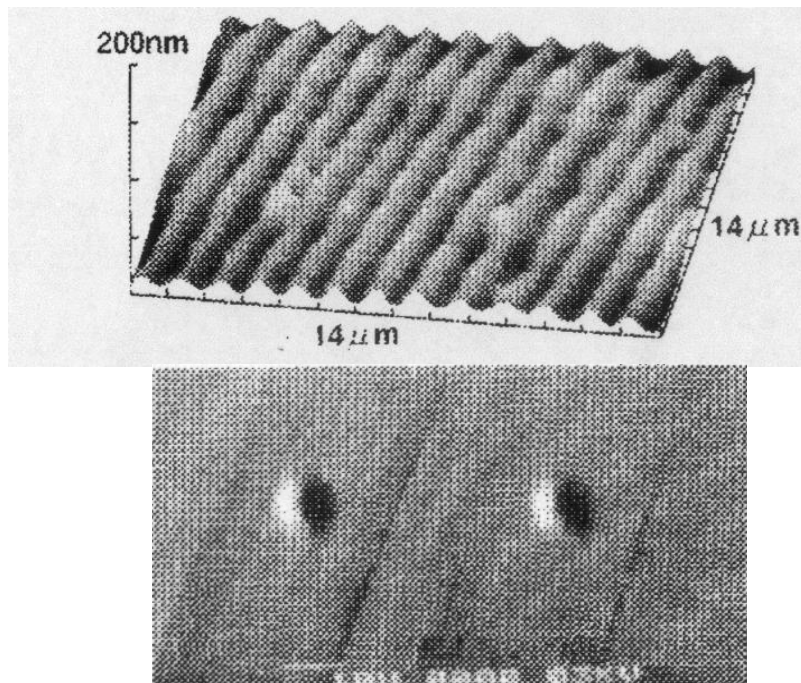
Under illumination the metastable system approaches equilibrium with excess Ag segregation.

Annealing at higher temperature allows Ag to dissolve again in the solid solution

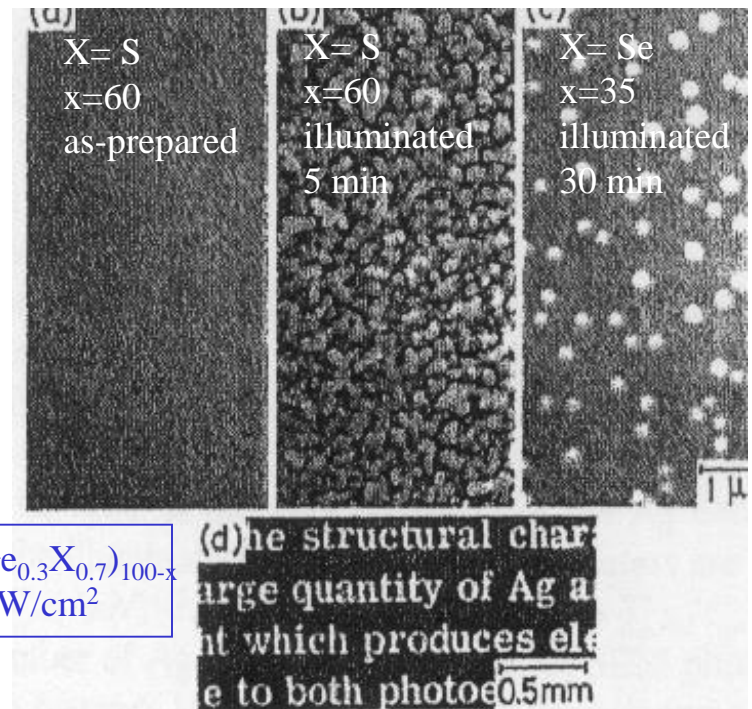
Application of photomigration-phodeposition

Increased reflectivity for Ag rich region
photoexpansion

Gratings/ microlenses



Optical memories



Au addition → increase in the photosensitivity of photodeposition by two orders of magnitude (Au clusters = nucleation centers for Ag)

T. Kawaguchi, K. Tanaka and S.R.Elliott; Handbook of advanced electronic and photonic Materials and devices AP, N.H Nalwa ed. (2001) p 91

Photocrystallisation (phase change)

Exist in chalcogenide with or without ion

Ge-Sb-Te (GST- $\text{Ge}_2\text{Sb}_2\text{Te}_5$)

Ag-In-Sb-Te (AIST)

Ordered state

Disordered state

crystalline
 AgSbTe_2

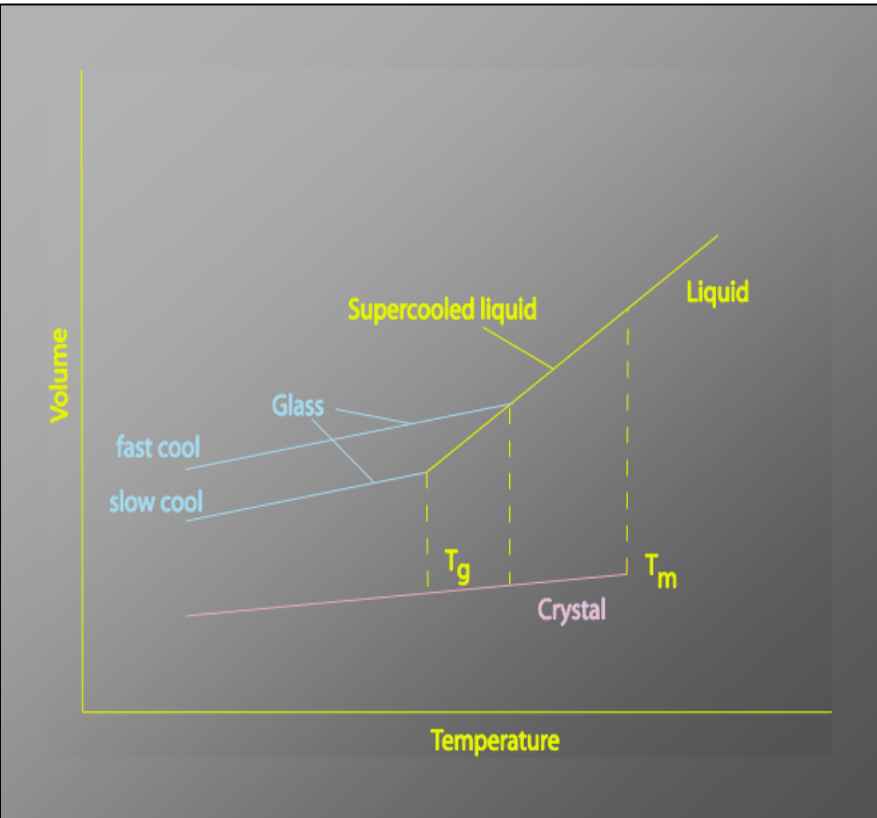
+
amorphous
In-Sb

amorphous
 AgSbTe_2

+
amorphous
In-Sb

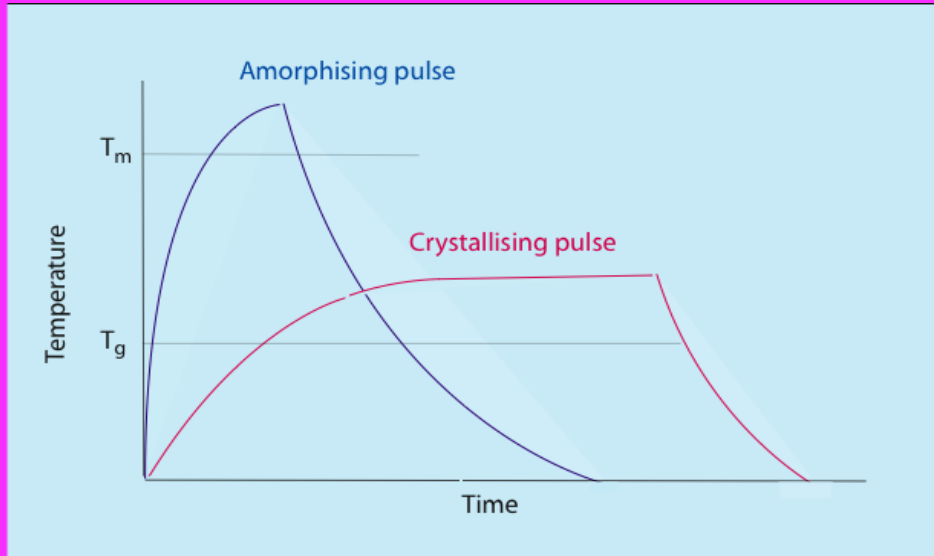
$h\nu$
laser beam

Critical cooling rate
3.4 K/ns



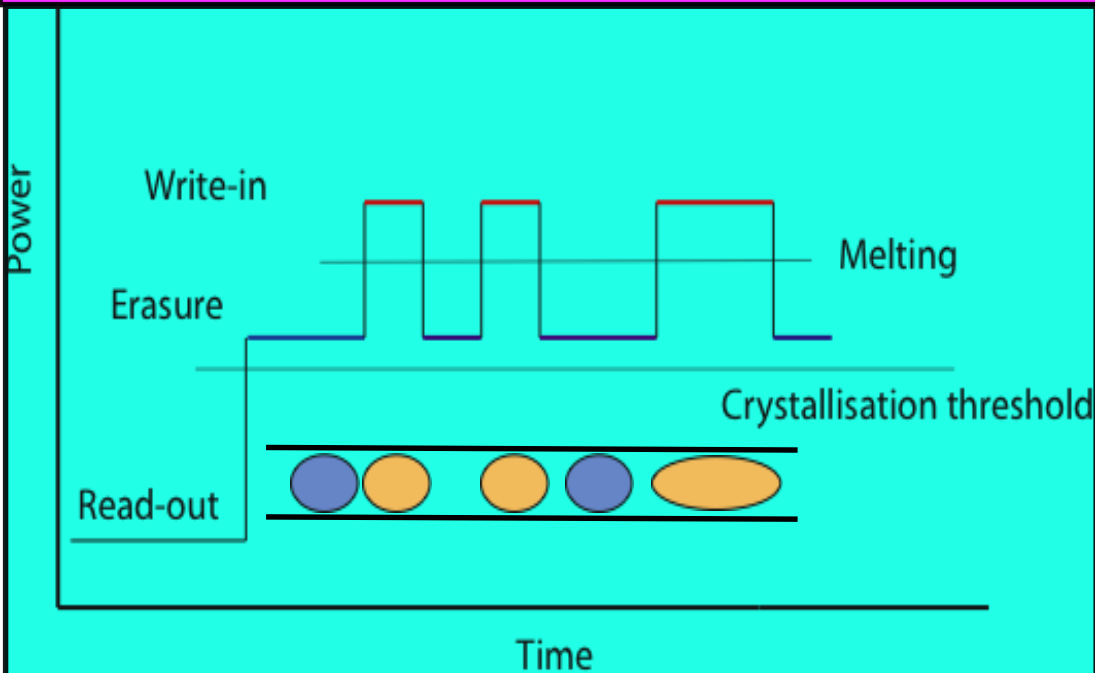
Different reflectivity for amorphous and crystalline AgSbTe_2

Application of photocrystallisation



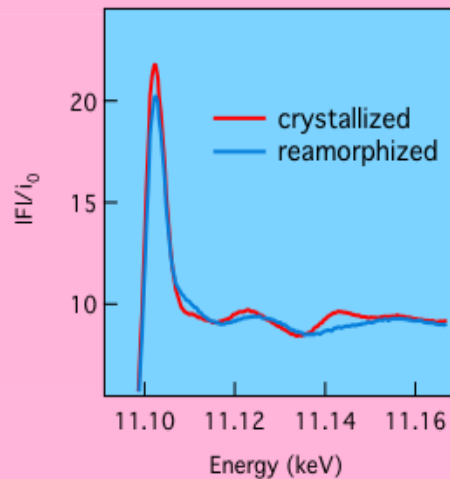
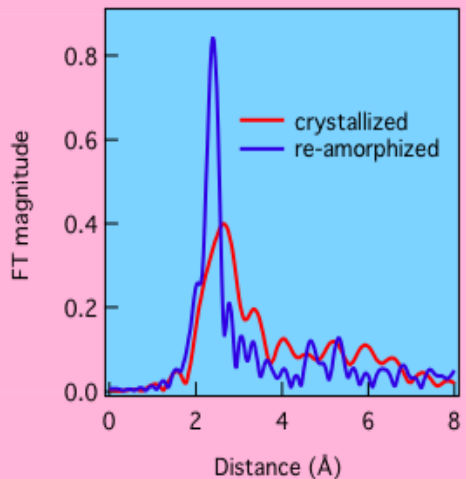
Rewritable optical disk
memory
Phase change:
Write/Erase phenomena

Laser-induced
annealing/melting



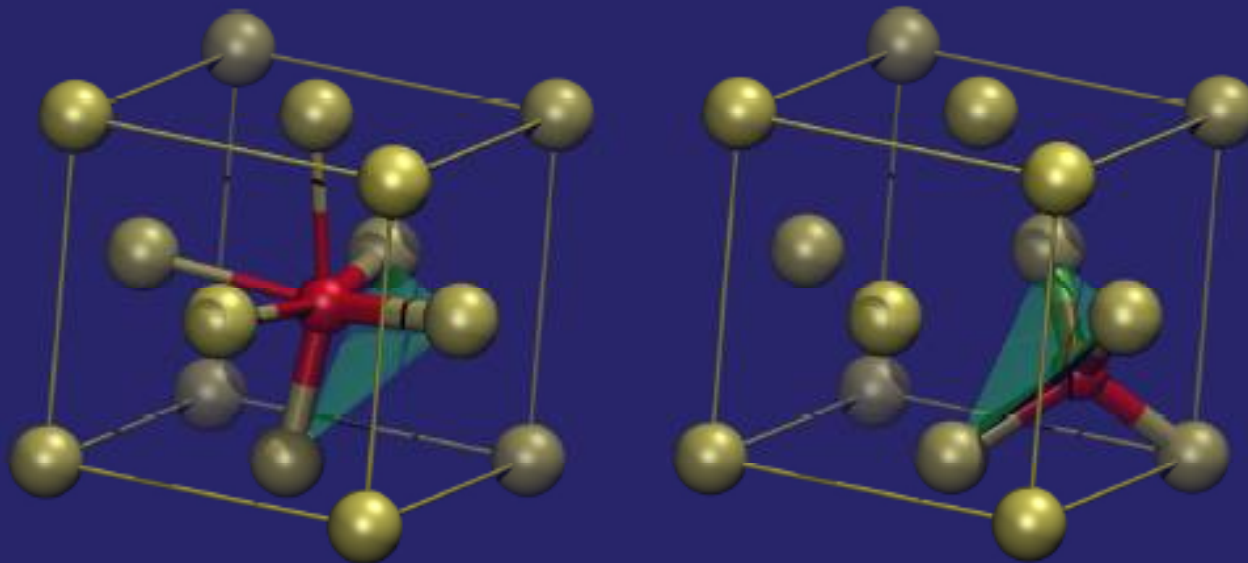
Pulse structure

Ge-edge data ($\text{Ge}_2\text{Sb}_2\text{Te}_5$)



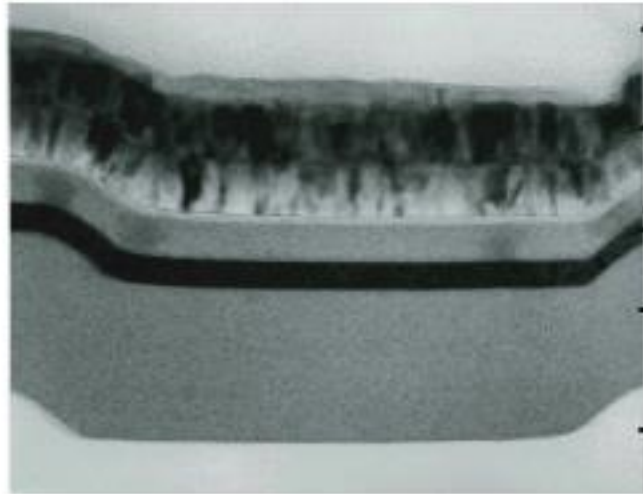
The transition between the crystalline and amorphous states can be viewed as an **umbrella-switch** of Ge atoms from a **octahedral to tetrahedral** symmetry position within the Te fcc sublattice

Very big change in EXAFS and XANES



A.Kolobov et al, 2004, Nature Mater. 3, 703

Real disc structure



UV resin

Reflection layer (heat sink)

Protection layer ZnS-SiO₂

Active layer (GST, AIST)

Protection layer ZnS-SiO₂

Polycarbonate disc

Fig. 6. Cross-sectional TEM observation of the basic 4-layer phase-change optical disk.

T. Ohta, JOAM 2001

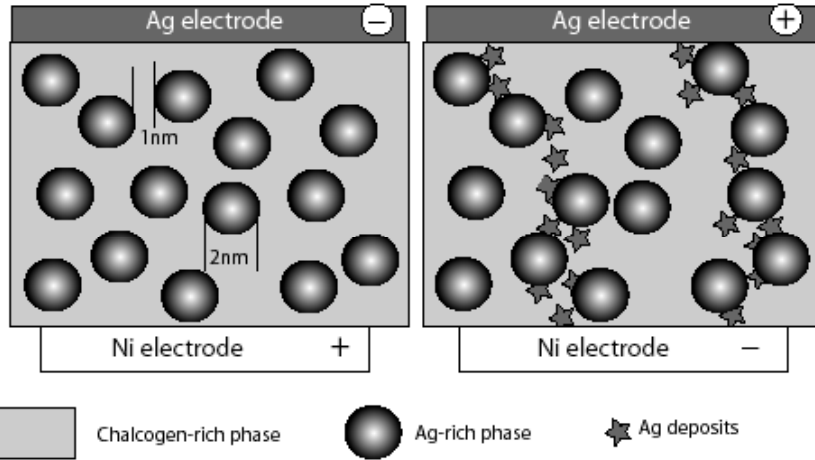
WHY PHOTOSTRUCTURAL CHANGES OCCUR ONLY IN AMORPHOUS CHALCOGENIDES?

- Excitation of lone-pair electrons is a trigger of the structural change - presence of **LP-electrons** is crucial - **group VI elements (chalcogens)**;
- Localization of photo-excited carriers and hence disorder is important - **amorphous**;
- **Low coordination number** is beneficial since it makes the structure floppy.

Amorphous chalcogenides are the only materials that satisfy all these requirements

Diffusion under \vec{E} and $h\nu$: PMC memories

« Programmable Metallization Cell Memory Devices »



☞ *bias* → accumulation of silver metal creating a conductive link (« on » state) - Ag is oxidised at the anode and reduced at the cathode

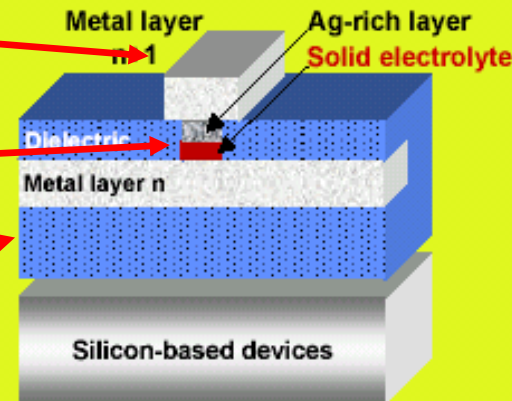
☞ Reversing the *bias* breaks down the silver and restore the initial resistive state (« off » state)

Anode: Ag
or Ag-containing material

Solid electrolyte:
Ag photodissolution
in $GeS(Se)_y$

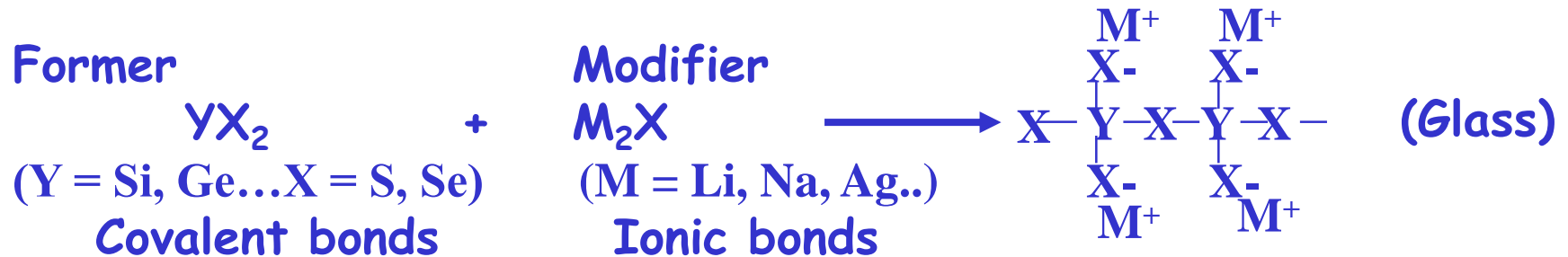
Cathode: inert metal
(Cr, Ni..)

Solid electrolyte is formed in a via between two levels of metal in a *back end of line (BEOL)* process



Ionic conductive chalcogenide glasses

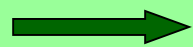
Glasses exist in large composition domains



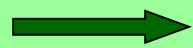
Ag (Na)- based chalcogenide glasses



Ag (Na) content varying
from 0.01 - 30 at%



evolution of conductivity with composition

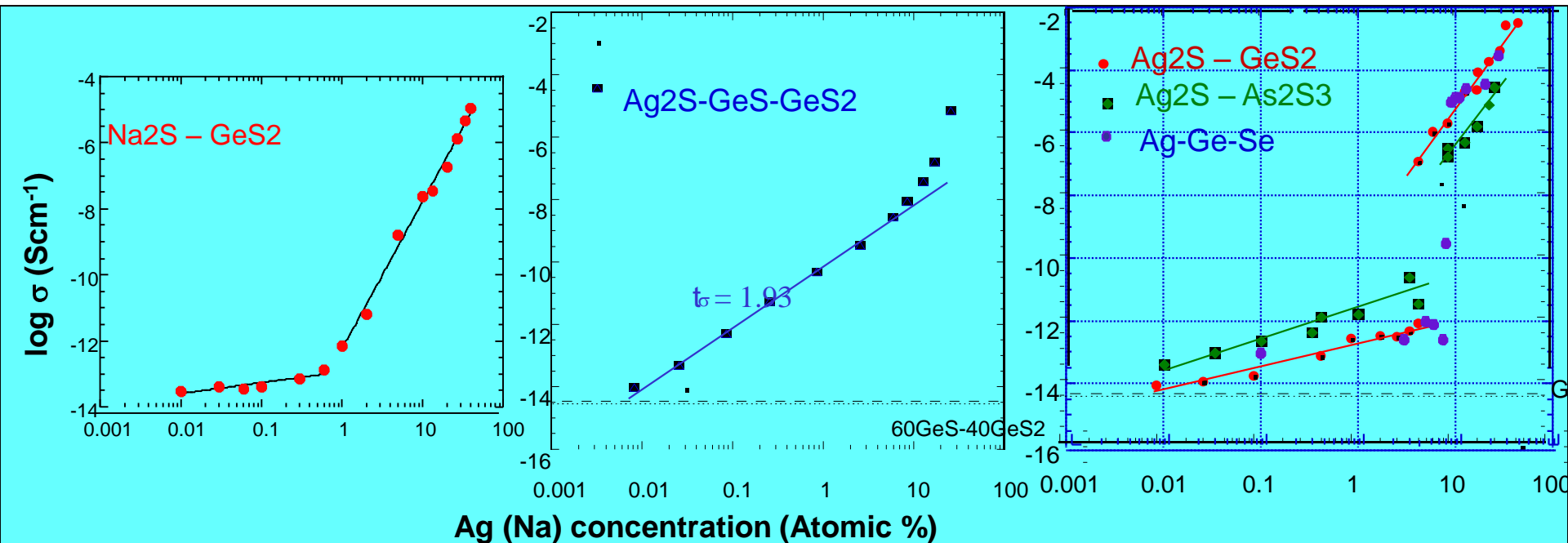


non-Arrhenius behaviour ($\log \sigma \propto 1/T$)

*M.Kawasaki, Kawamura J, Y. Nakamura and M. Aniya; SSI 123 (1999) 259

M.A. Urena, A.A Piarristeguy. M. Fontana and B. Arcondo; SSI 176 (2005) 505

Variation of conductivity (298 K) with Ag(Na) content (at %) in Ag(Na)-X-Y glasses (X=Ge,As; Y=S,Se)



Ag (Na) concentration (Atomic %)

A. Pradel, N. Kuwata, M. Ribes, 2003, J.Phys.: Cond. Mat. 15, S1561; M.A. Urena, A.A Piarristeguy, M. Fontana and B. Arcondo; SSI 176 (2005) 505

3 different behaviours

- $\text{Na}_2\text{S} - \text{GeS}_2$: Change in the transport regime at about 1 at % in sodium (electronic to ionic ?)
- $\text{Ag}_2\text{S} - \text{GeS} - \text{GeS}_2$ and Ag-based glasses: Change in the transport regime at about 5-8 at % in silver
- Ag-based glasses: large increase of 4-5 orders of magnitude in the conductivity at about 5-8 at % in silver

Ag₂S-GeS-GeS₂ and Ag-based glasses
Structural studies (microscopic, nanoscopic scale)

FE-SEM (Field Effect - Scanning Electron Microscopy)

Chemical inhomogeneities

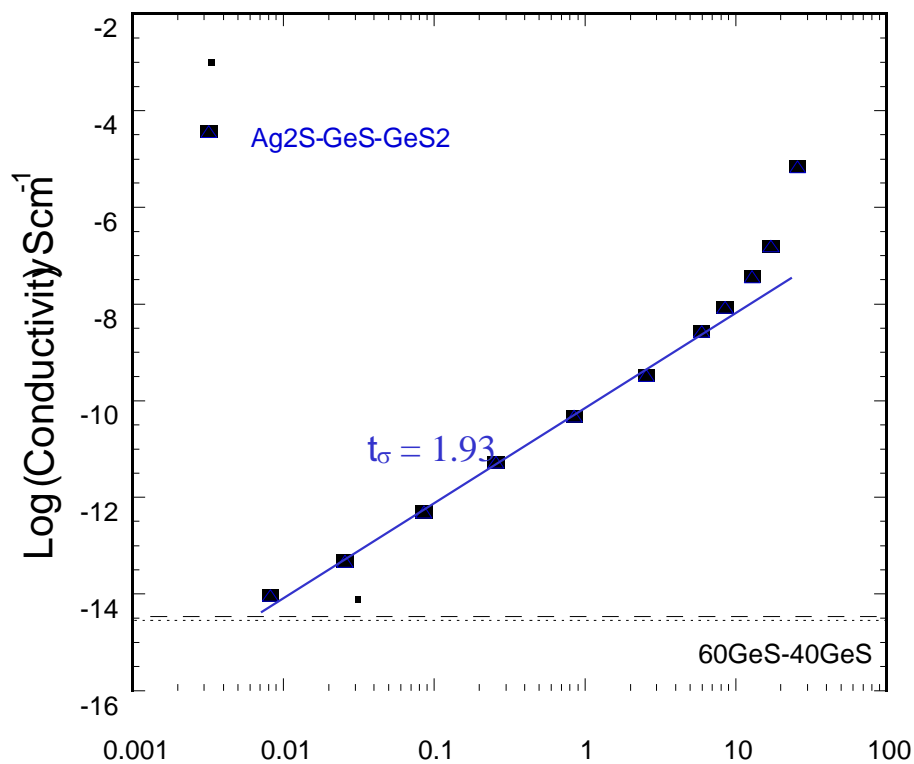
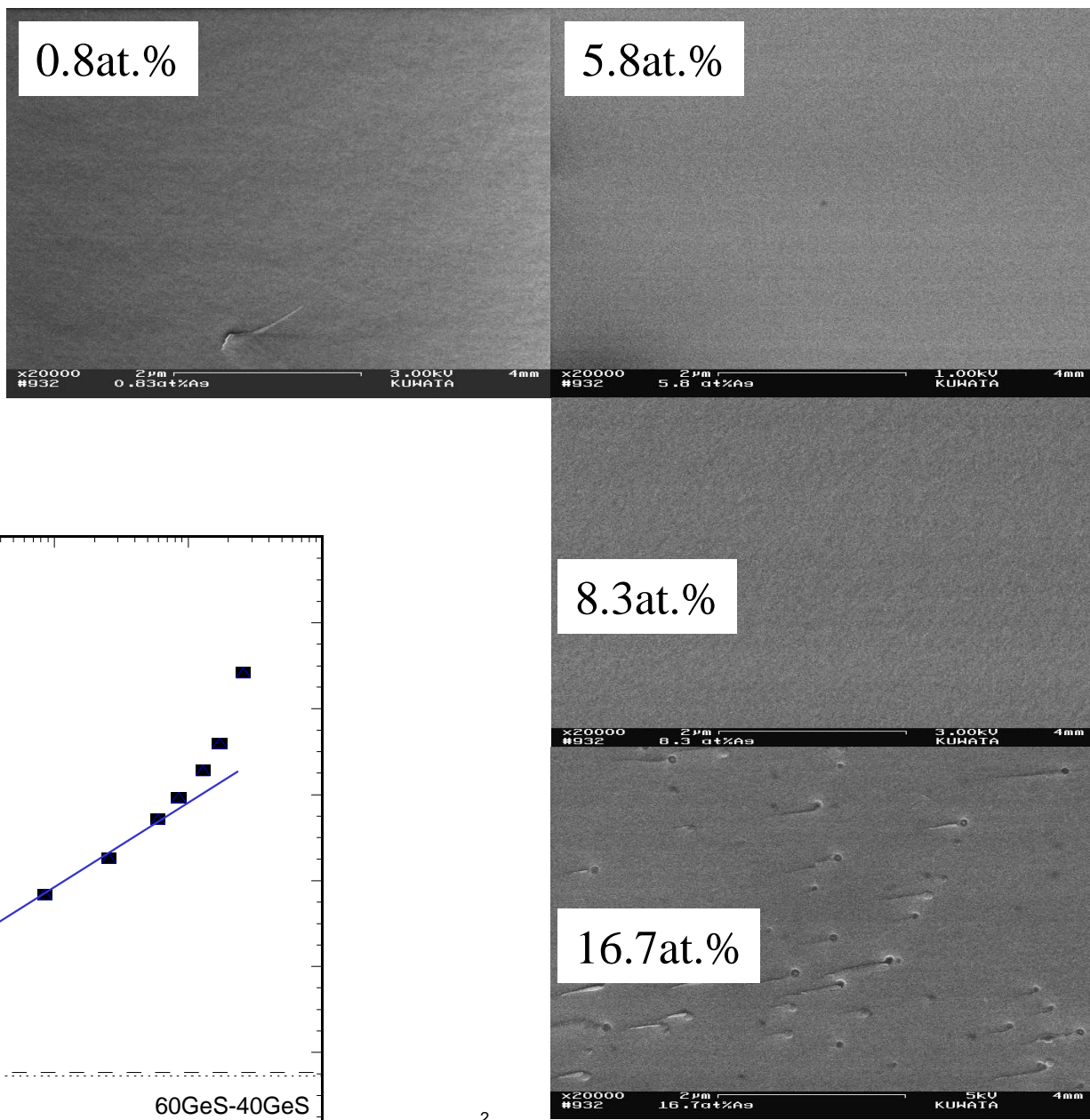
**EFM (Electric Force Microscopy) Surface potential imaging
and surface electric modification**

Electrical inhomogeneities

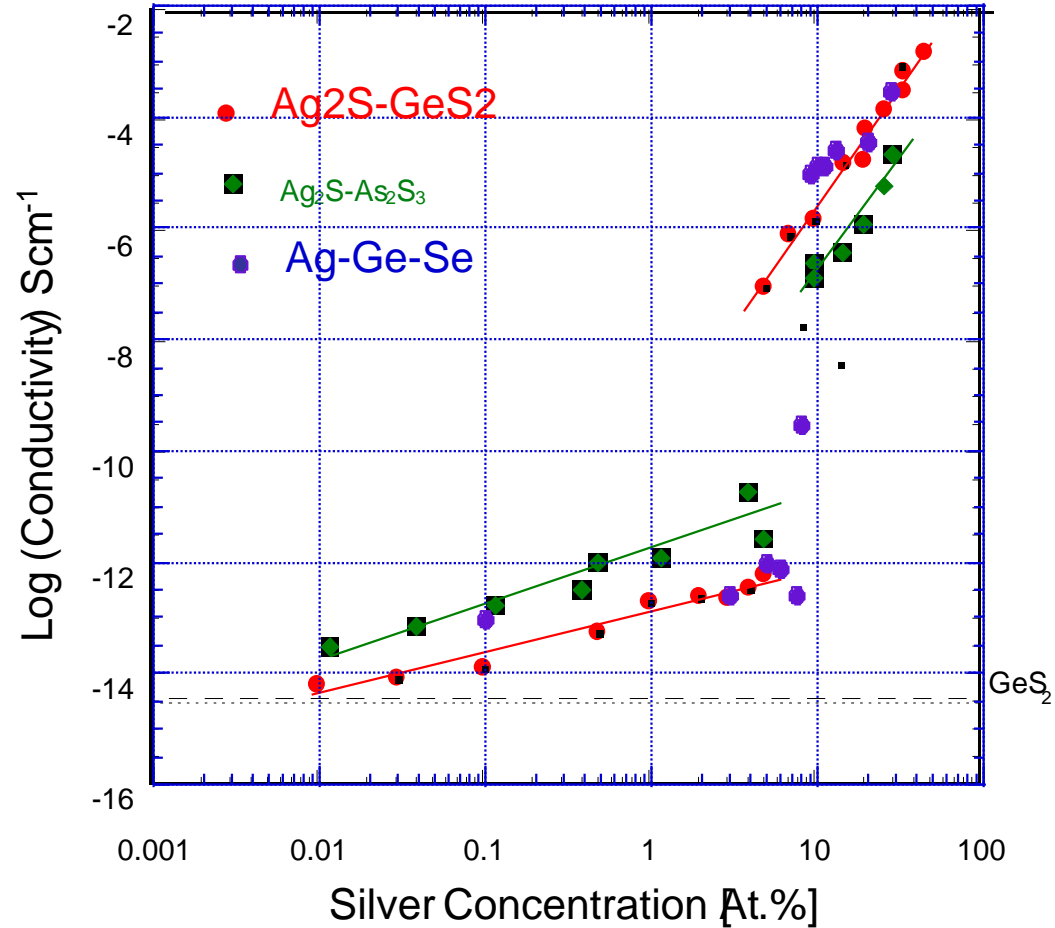
FE-SEM
(LEO-982)

$Ag_2S-GeS-GeS_2$

No
phase separation



Ag-based glasses showing a large increase (4-5 orders of magnitude) in the conductivity at about 5-8 at % in silver



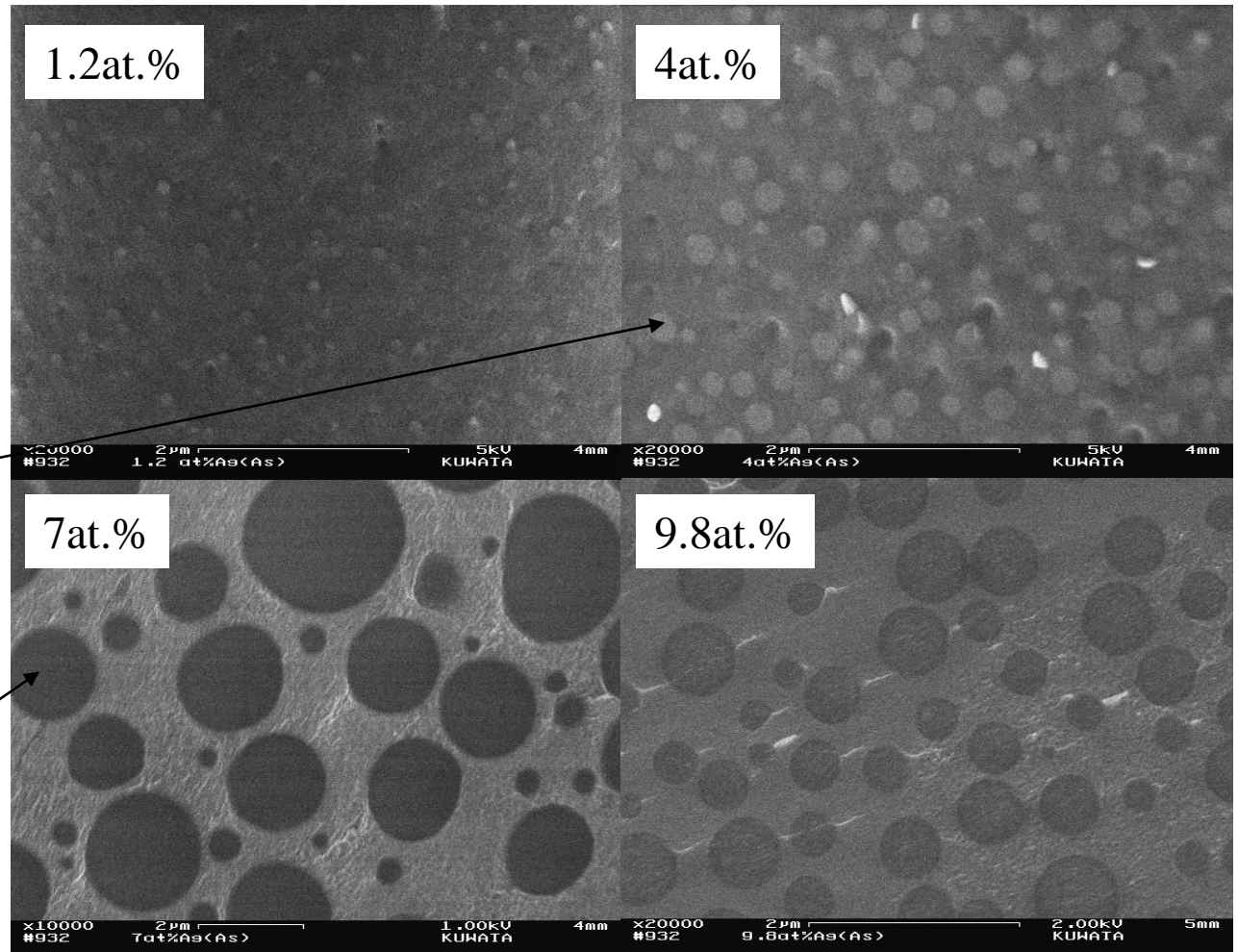
FE-SEM
(LEO-982)



Glasses are
phase separated

Ag-rich phase

Ag-poor phase



the change in the conductivity regime occurs
when the Ag-rich phase starts connecting

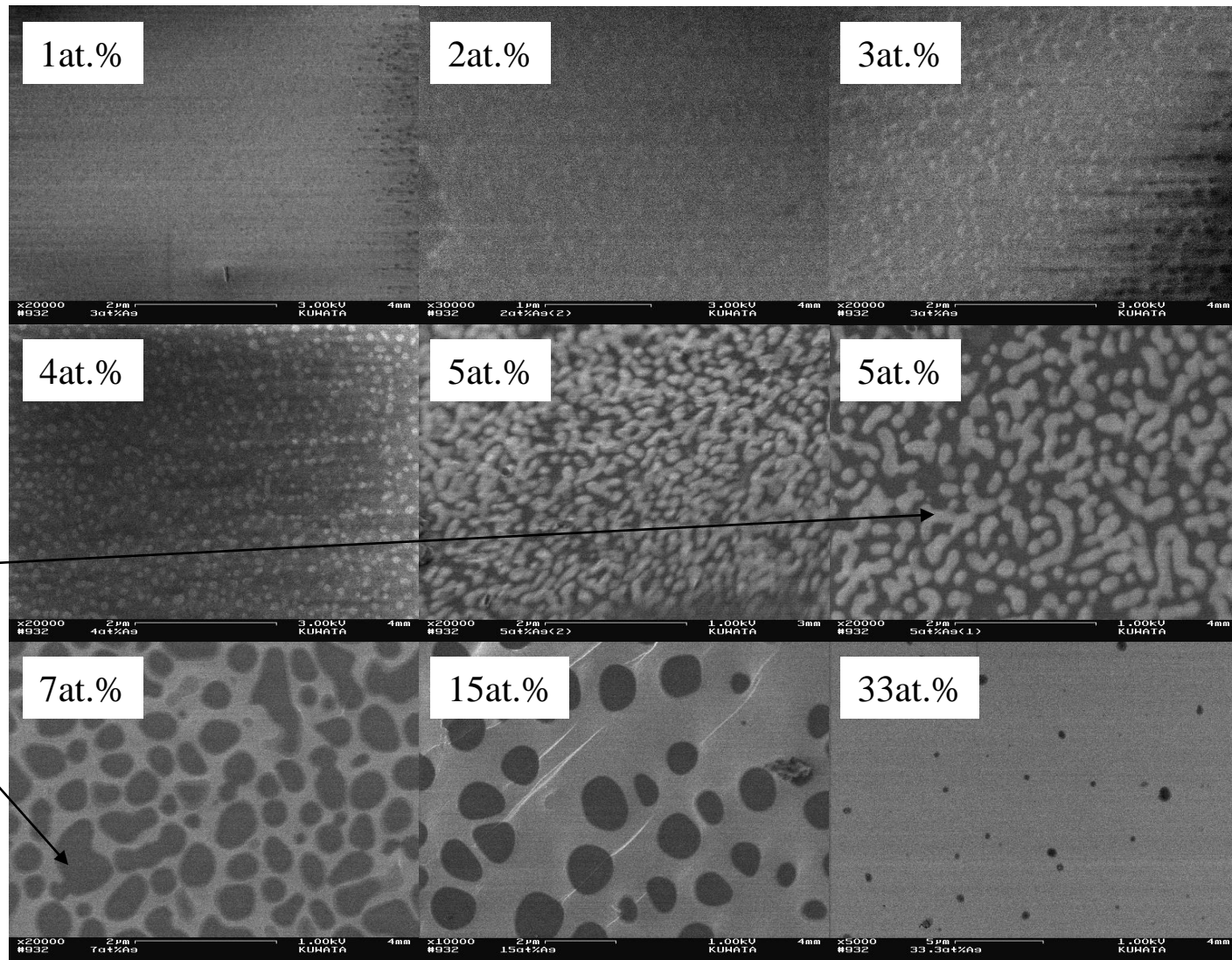
FE-SEM
(LEO-982)

$\text{Ag}_2\text{S} - \text{GeS}_2$

Glasses are
phase
separated

Ag-rich phase

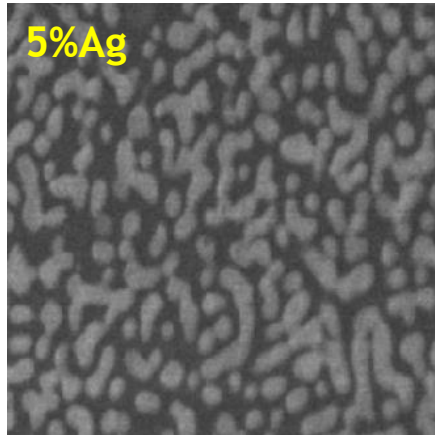
Ag-poor phase



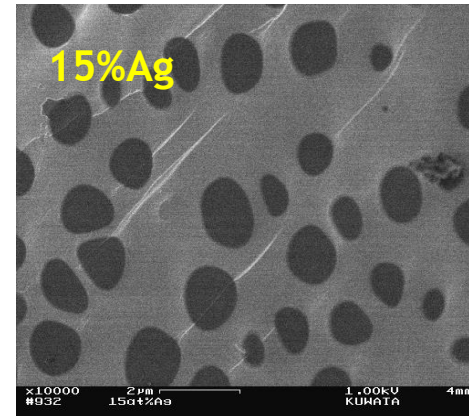
the change in the conductivity regime occurs
when the Ag-rich phase starts connecting

Comparison FE-SEM / EFM (Ag₂S-GeS₂ glasses)

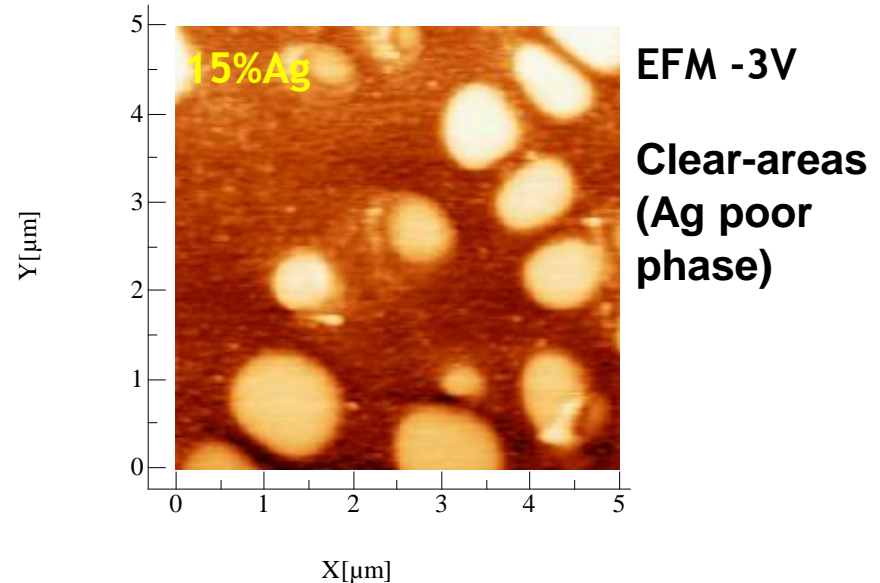
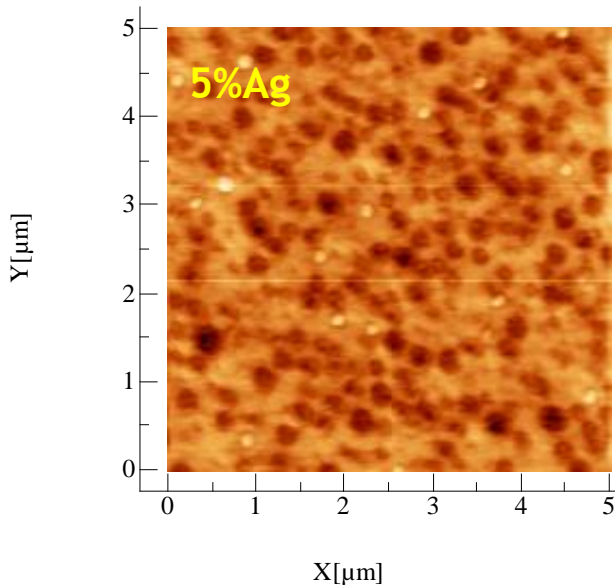
- Weak conductivity domain : Ag-poor phase connected
- High conductivity domain : Ag-rich phase connected



Clear areas
(Ag-rich
phase)
d~0,3 μ m

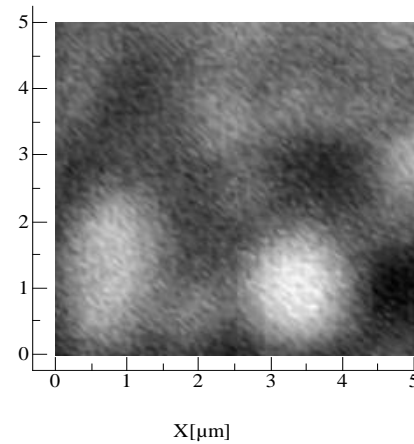
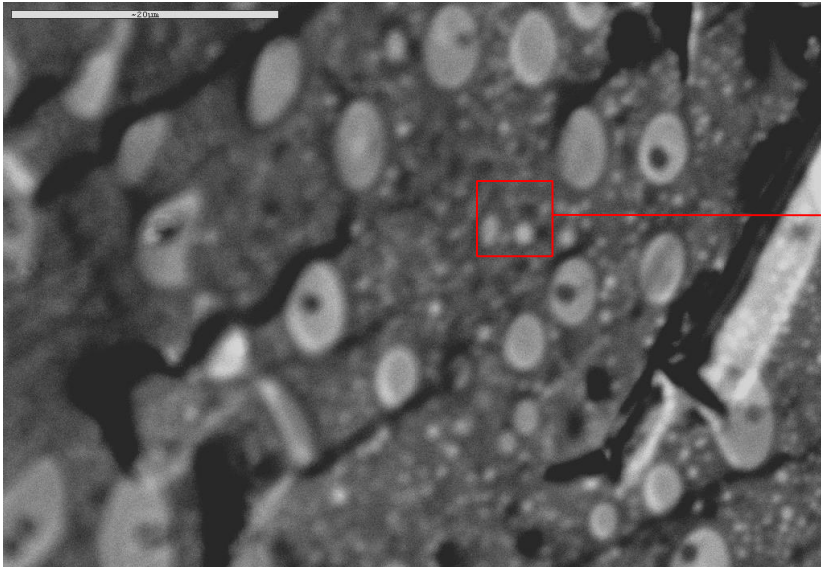


Dark areas
(Ag-poor
phase)
d~0,8-0,9 μ m



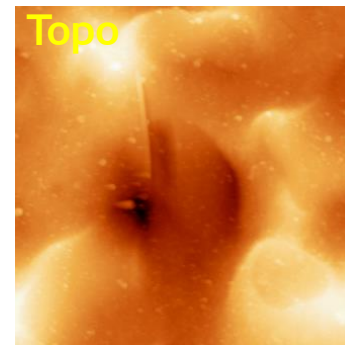
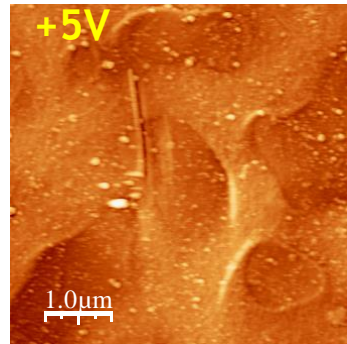
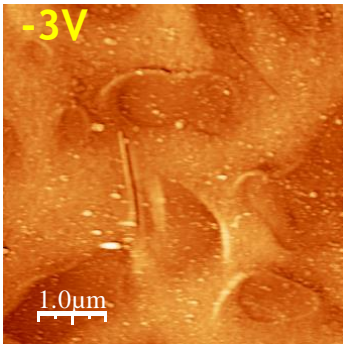
$(\text{Ge}_{25}\text{Se}_{75})\text{Ag}:10\%$

Electrons retrodiffusés



Clear areas (Ag-rich phase in a Ag-poor matrix)

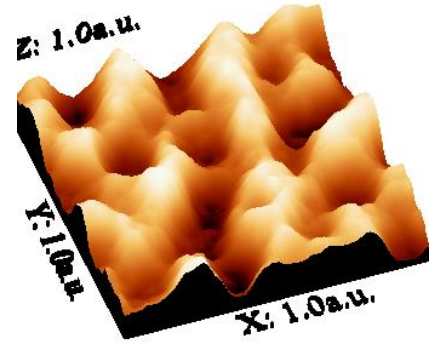
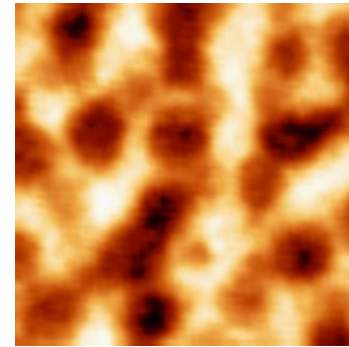
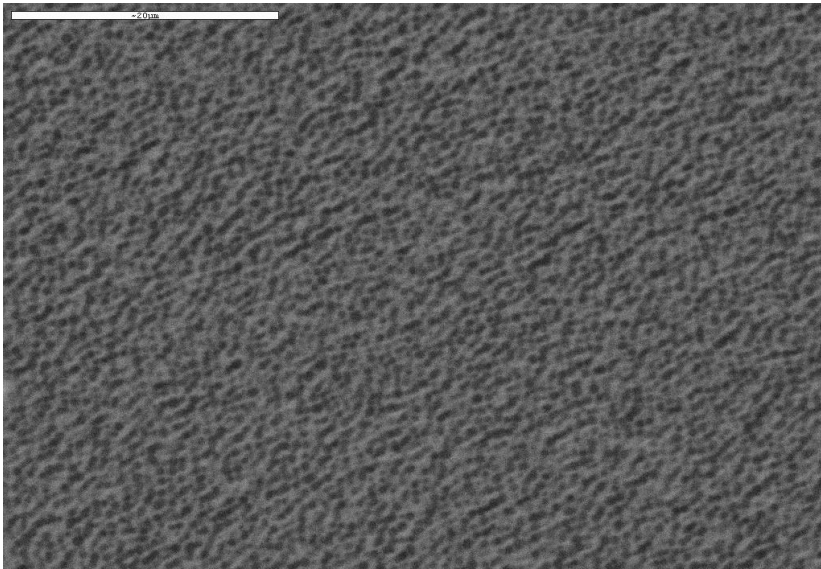
EFM



Dark areas in a clear matrix but a weaker contrast !

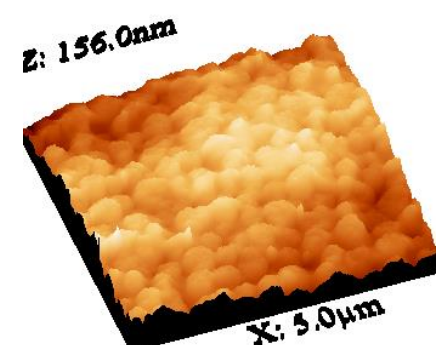
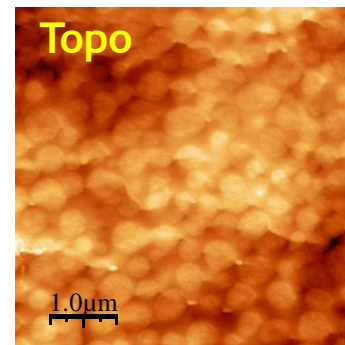
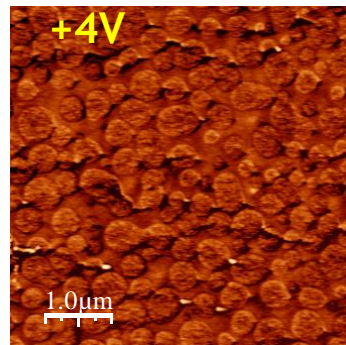
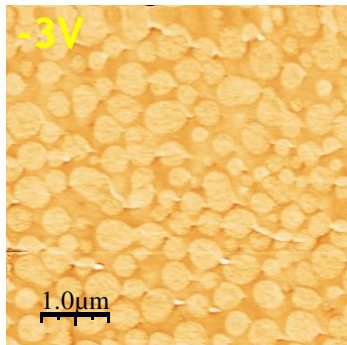
$(\text{Ge}_{25}\text{Se}_{75})\text{Ag}:15\%$

Electrons retrodiffusés



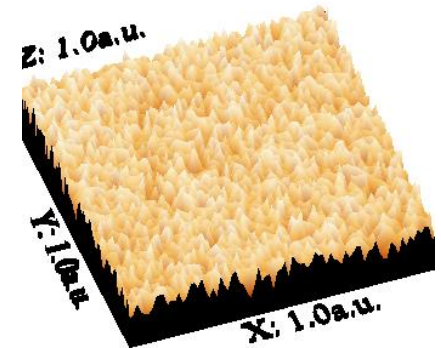
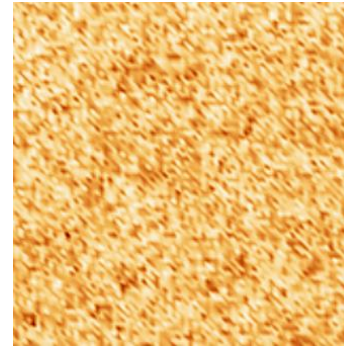
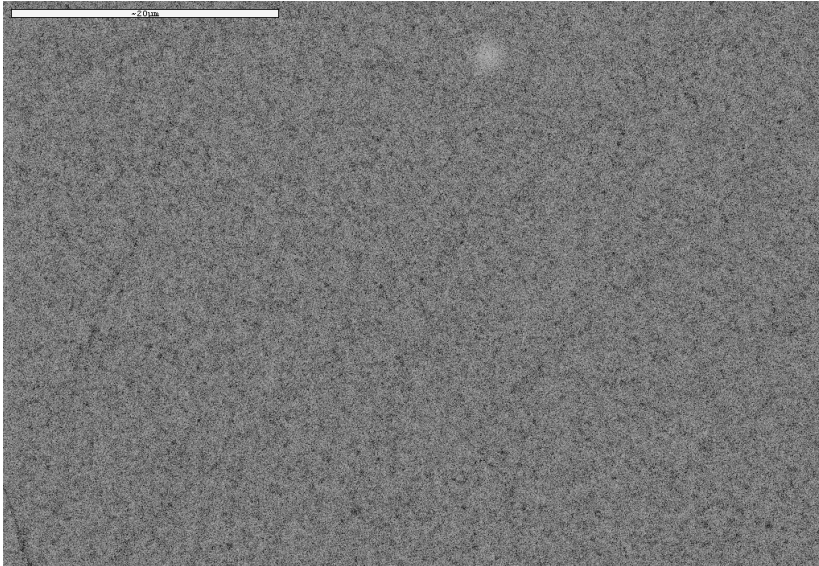
d ~ 1 μm

EFM

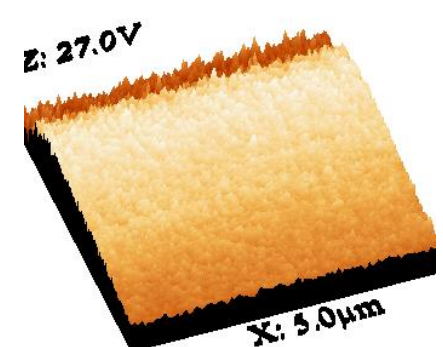
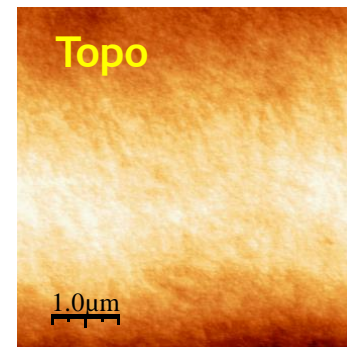
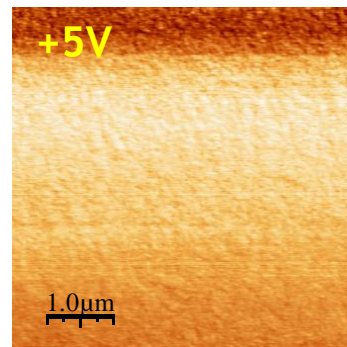
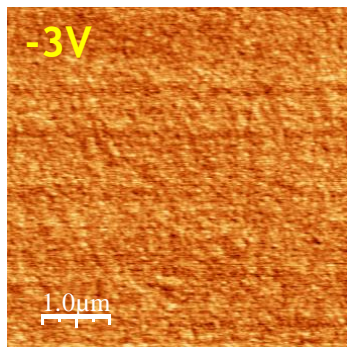


$(\text{Ge}_{25}\text{Se}_{75})\text{Ag}:25\%$

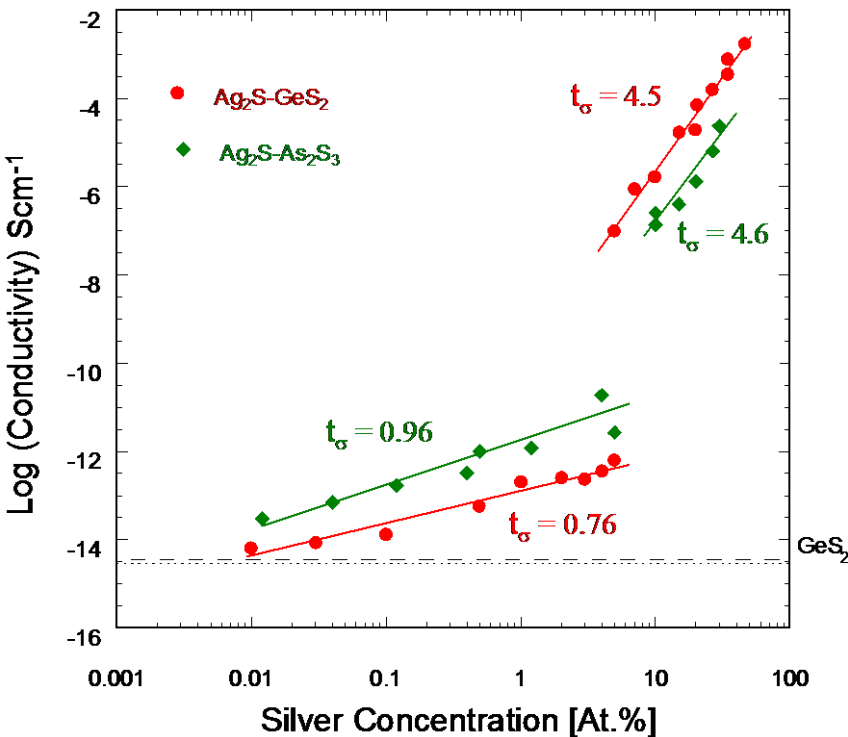
Electrons retrodiffusés



EFM



Variation of conductivity (298 K) with Ag content (at %) in $\text{Ag}_2\text{S} - \text{GeS}_2$ and $\text{Ag}_2\text{S} - \text{As}_2\text{S}_3$ glasses



The glasses are phase separated

The jump in the conductivity occurs when the phase previously embedded in the connecting phase becomes the connecting one

percolation threshold with the Ag-poor phase (Ag-rich phase) being responsible for the conductivity at low silver (high silver) content

At low Ag content, power law dependence: $\sigma = Cx^{t_\sigma}$

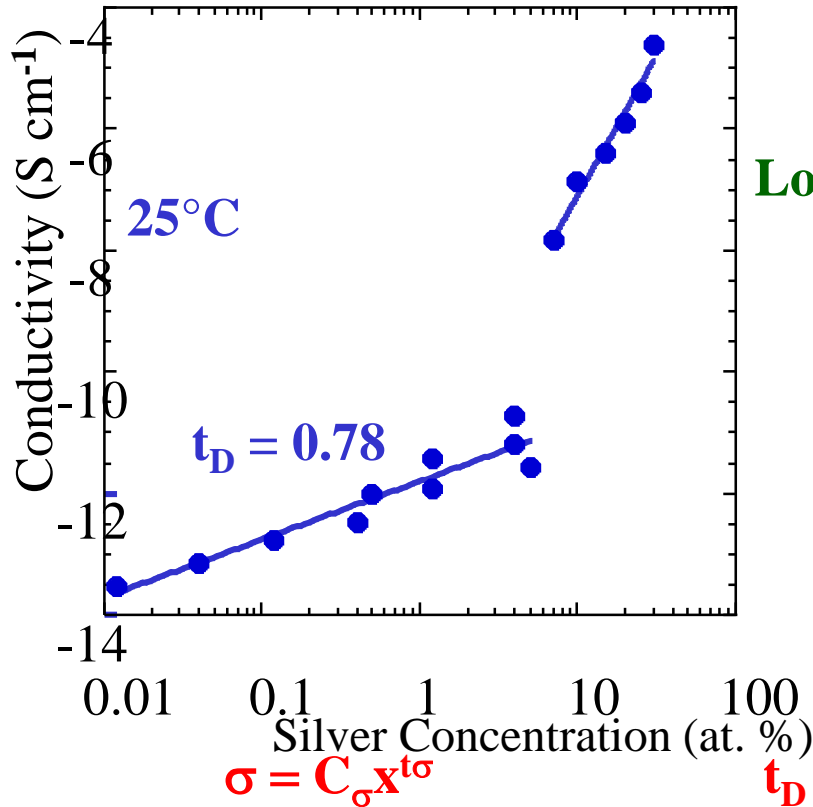
Nature of the charge carriers (electrons to ions)?

EMF <---> Tracer diffusion coefficient

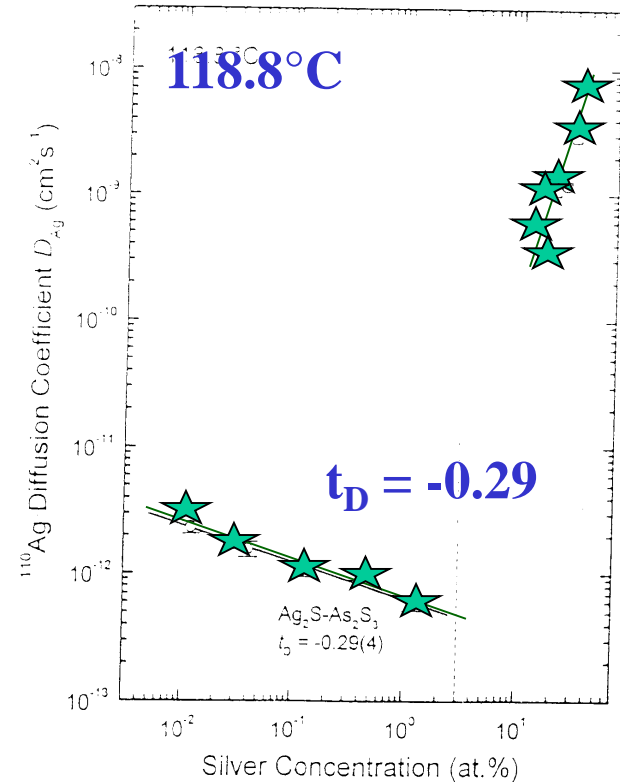
Ag₂S - As₂S₃ glasses

Conductivity

¹¹⁰mAg tracer diffusion coefficient



Log-log plots



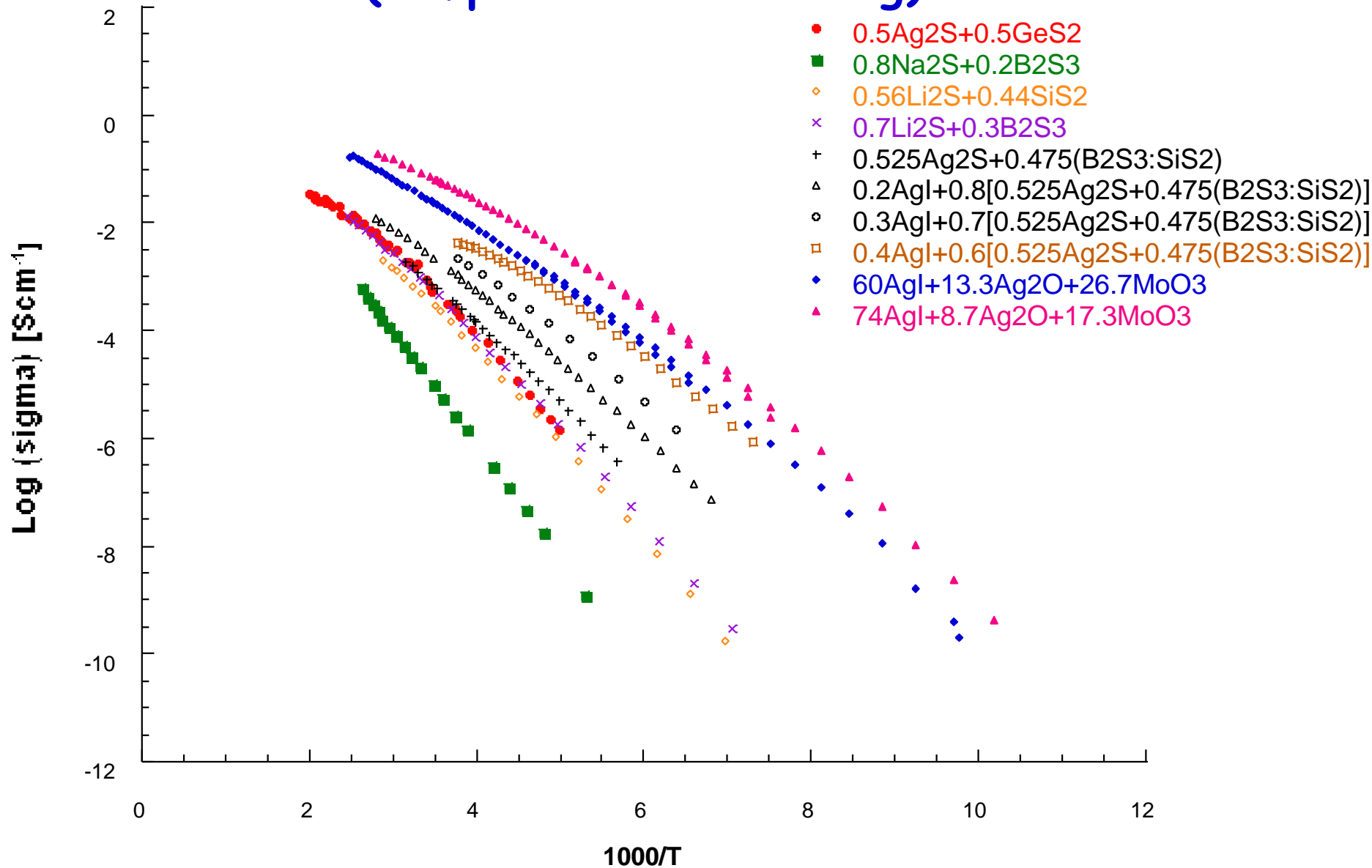
low silver content: conductivity mainly ionic $D = C_D x^{t_D}$
 high silver content: conductivity purely ionic $t_\sigma > 0.99$
 (same conclusions for: Ag₂S-GeS₂ and Ag₂S-GeS-GeS₂)

Bychkov E, Tsegelnik V, Vlasov Y, Pradel A and Ribes M., JNCS 208 (1996) 1.

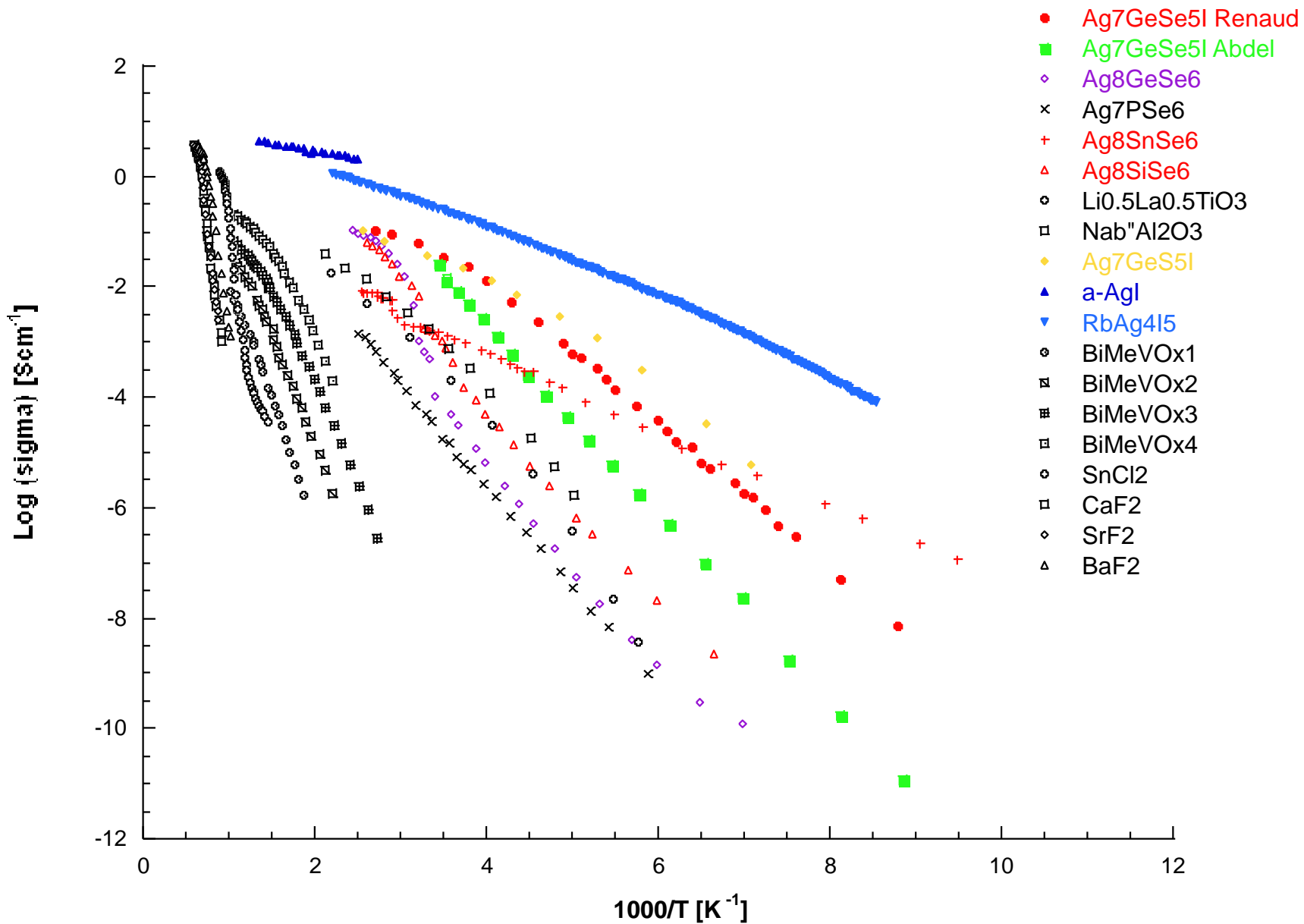
Bychkov E, Bychkov A, Pradel A and Ribes M., SSI 113-115 (1998) 691.

**Non-Arrhenius behaviour ($\log \sigma \propto 1/T$)
in glasses and more generally
in super-ionic conductors**

Arrhenius plots of σ for different « superionic » glasses (temperatures below T_g)



Arrhenius plots of σ for different « superionic » Crystallised phases



Because of super-Arrhenius behaviour below T_g in glasses one can think that it exists a « Mobile ion » glass transition

Such a transition cannot be observed easily because its weakness. (To date it has only been reported by Hahashi and Ojuni - $\text{AgPO}_3\text{-AgI}$ glass at $\sim 80\text{K}$).

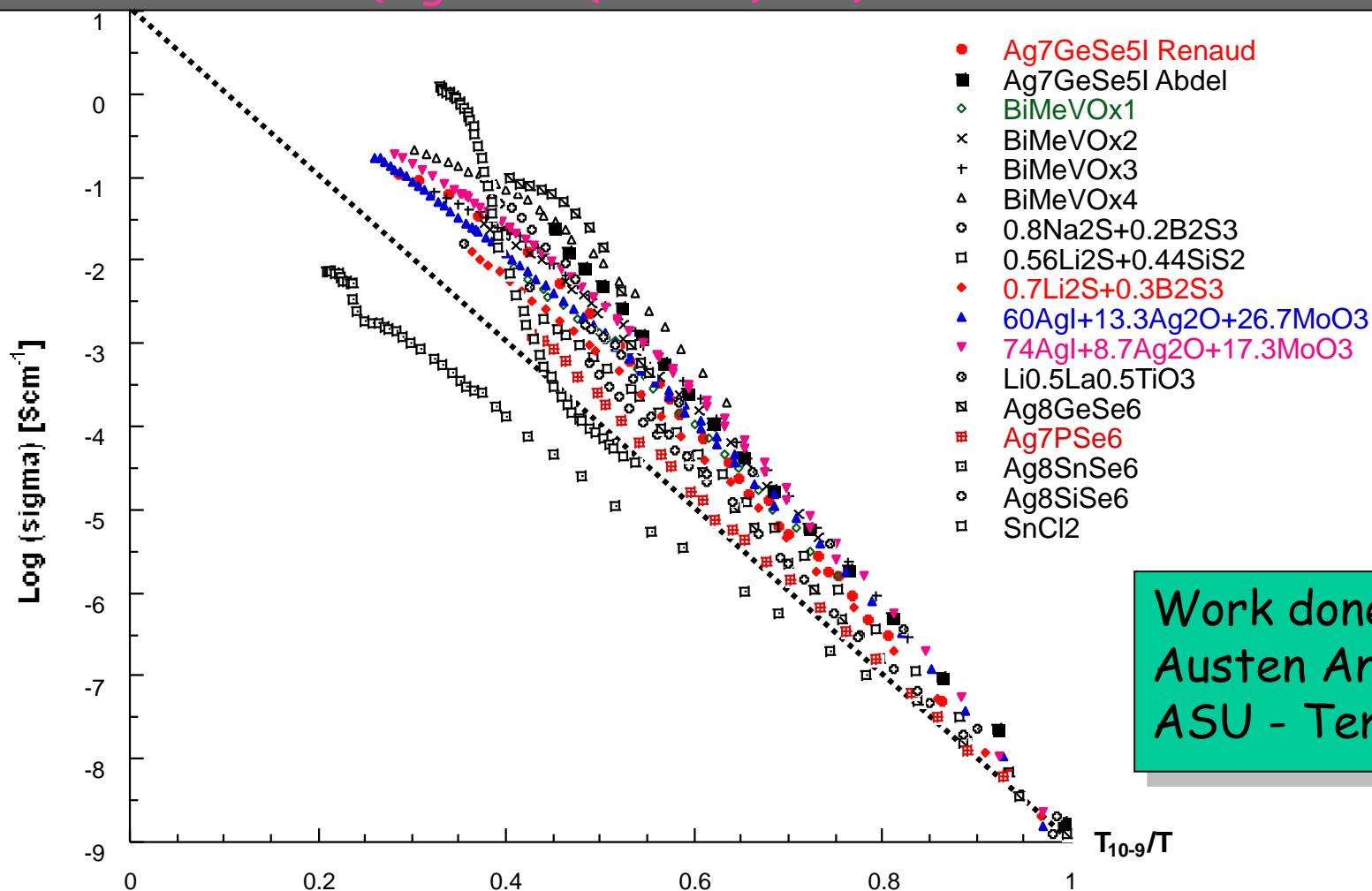
It is also possible to imagine a « mobile ion T_g » for superionic crystalline compounds with disorder in the mobile ion sub-lattice (for temperature higher than this hypothetical temperature ions move in a quasi-liquid sub-lattice)

F

For temperature greater than that of « mobile ion T_g » cooperative cation motions \rightarrow super-Arrhenius behaviour

Scaled Arrhenius plots of σ for different « superionic » Glass and Crystalline compounds

In the absence of experimental data one can tentatively take for « mobile ion T_g » the temperature where the conductivity is about 10^{-9} Scm^{-1} , allowing a *scaling* of the variation of the conductivity
 $(\log \sigma \propto T(\sigma = 10^{-9}) / T)$



Work done with
Austen Angell
ASU - Tempe

***STOP** pour le moment*